A Theoretical Study of Collinear Scattering:

I. A New Method to Calculate Reactive and Dissociative Cross Sections of Atom Plus Diatom Systems

II. A Reexamination of the Collinear Inelastic Collision of Two Diatomics

Thesis by

John Patrick Dwyer

In Partial Fulfillment of the
Requirements for the Degree of
Master of Science

California Institute of Technology
Pasadena, Ca. 91125

1976

(Submitted June 1, 1976)

ACKNOWLEDGMENTS

I would like to thank my advisor, Dr. Aron Kuppermann, whose advice and unflagging support made this work possible.

I would also like to thank Ambassador College for the use of their computer facilities.

TABLE OF CONTENTS

	Page
Part I	3
Appendix A	24
Appendix B	29
Part II	49

Abstract

In attempting to understand the nature of a chemical reaction, the theoretical chemist is severely limited. Exact quantum mechanical (EQM) 3-D calculations of all but the simplest chemical systems are prohibitively expensive. In addition, accurate potential surfaces are not available for most reactions. Finally, because the cost of computation increases with the collision energy, 3-D investigations are restricted to low energies. To circumvent these difficulties, one might develop approximate theories, or do exact calculations on model systems. The first method permits one to calculate cross sections for real chemical reactions, but it leaves one wondering if the results are correct, since experimental work is often not sophisticated enough to verify (or disclaim) them. The second method has the disadvantage of being "unreal". Cross sections for model systems may exhibit properties not found in the real system, while hiding or distorting properties which actually exist. However, EQM calculations on model systems are useful for testing approximate theories.

In this thesis we present two calculations on model systems. The first is for the collinear collision of H and H_2 using a realistic potential surface. Although other investigations have calculated reactive and nonreactive cross sections for atom-diatom collisions, their results have been restricted to low energies and have not included dissociation as a possible reaction pathway. We present a general method for calculating reactive, nonreactive and dissociative cross sections for an atom-diatom collision and apply it to the H_3 surface.

In part II we present transition probabilities for the nonreactive collinear collision of two identical diatoms. We use a model potential surface, but are able to compare our results to those of other investigators who used an approximate theory.

PART I

1. Introduction

There have been several efforts[1] to calculate exact quantum mechanical cross sections for collinear reactions. Usually these reactions are of the form

$$A + BC \rightarrow AB + C,\ A + BC.$$

In general the calculated wavefunctions have not included contributions from the continuum, i.e., dissociation. In order to achieve convergence, only collision energies significantly smaller than dissociation energies have been used.

Three questions immediately arise. What are the cross sections for higher energies? Does the continuum affect reactive and nonreactive cross sections, and to what degree? What are the cross sections for dissociation? In sections 2 and 3 we present a general method to calculate reactive, nonreactive and dissociative cross sections for the collinear collision of A and BC. The effects of the closed (or open) continuum states are included naturally. In section 4 we examine the unusual nature of some of these cross sections. Finally, in section 5, we present results for collinear $H + H_2$ using a realistic potential surface.

2. Coordinate Systems and Matrix Equations

Consider the collinear arrangement of A, B and C where ξ_A, ξ_B and ξ_C are the laboratory coordinates. The Hamiltonian for this

system is

$$H = -\frac{\hbar^2}{2m_A}\frac{\partial^2}{\partial \xi_A^2} - \frac{\hbar^2}{2m_B}\frac{\partial^2}{\partial \xi_B^2} - \frac{\hbar^2}{2m_C}\frac{\partial^2}{\partial \xi_C^2} + V(\xi_A, \xi_B, \xi_C). \quad (1)$$

If we let

$$r_1 = \xi_B - \xi_A,$$

$$r_2 = \xi_C - \xi_B$$

$$\text{and } R = \frac{m_A \xi_A + m_B \xi_B + m_C \xi_C}{(m_A + m_B + m_C)},$$

the Hamiltonian becomes

$$H = -\frac{\hbar}{2}\left[\frac{1}{m_A}\frac{\partial^2}{\partial r_1^2} + \frac{1}{m_B}\left(\frac{\partial^2}{\partial r_1^2} + \frac{\partial^2}{\partial r_2^2} - 2\frac{\partial^2}{\partial r_1 \partial r_2}\right) + \frac{1}{m_C}\frac{\partial^2}{\partial r_2^2} + \frac{1}{M}\frac{\partial^2}{\partial R^2}\right]$$

$$+ V(r_1, r_2), \quad (2)$$

where $M = m_A + m_B + m_C$. The wavefunction is given by

$$H\Psi = \mathcal{E}\Psi \quad (3)$$

where $\mathcal{E}$ is the total energy. If we let T_{cm} be the kinetic energy of the center of mass and set

$$H = H_0 + H_1, \quad (4)$$

where

$$H_1 = -\frac{\hbar^2}{2M}\frac{\partial^2}{\partial R^2} ,$$

we get

$$\Psi(r_1, r_2, R) = \psi(r_1, r_2)e^{ikR} , \tag{5}$$

where

$$T_{cm} = \frac{\hbar^2 k^2}{2M}$$

and

$$H_1\Psi = T_{cm}\Psi .$$

Now let

$$x_2 = r_2$$

$$\text{and } x_1 = r_1 + \frac{\mu_{BC}}{m_B} r_2 ,$$

where

$$\mu_{BC} = \frac{m_B m_C}{m_B + m_C} .$$

x_1 is the distance between A and the center of mass of BC. The new Hamiltonian, H_0, becomes

$$H_0 = -\frac{\hbar^2}{2\mu_{A,BC}}\frac{\partial^2}{\partial x_1^2} - \frac{\hbar^2}{2\mu_{BC}}\frac{\partial^2}{\partial x_2^2} + V(x_1, x_2) ,$$

where

$$\mu_{A,BC} = \frac{m_A(m_B + m_C)}{M} .$$

We now apply a coordinate transformation first proposed by Delves[2] and Hirschfelder and Jepsen.[3] Let

$$x_1' = \left(\frac{\mu_{A,BC}}{\mu_{BC}}\right)^{\frac{1}{4}} x_1$$

and $$x_2' = \left(\frac{\mu_{BC}}{\mu_{A,BC}}\right)^{\frac{1}{4}} x_2 .$$

Then we have

$$H_0 = -\frac{\hbar^2}{2\mu}\left(\frac{\partial^2}{\partial x_1'^2} + \frac{\partial^2}{\partial x_2'^2}\right) + V(x_1', x_2') \qquad (6)$$

where

$$\mu = (\mu_{A,BC}\,\mu_{BC})^{\frac{1}{2}}$$

$$= (\mu_{AB,C}\,\mu_{AB})^{\frac{1}{2}}$$

$$= [(m_A m_B m_C)/M]^{\frac{1}{2}} .$$

The Hamiltonian, as developed, is well suited for the arrangement channel A + BC, because one of the coordinates, x_2', is a measure of the internuclear distance of BC. To describe the other arrangement channel we need a new set of coordinates z_1', z_2' such that

$$z_1 = r_2 + \frac{\mu_{AB}}{m_B} r_1 ,$$

$$z_2 = r_1 ,$$

$$z_1' = \left(\frac{\mu_{AB,C}}{\mu_{AB}}\right)^{\frac{1}{4}} z_1$$

and $$z_2' = \left(\frac{\mu_{AB}}{\mu_{AB,C}}\right)^{\frac{1}{4}} z_2 .$$

The Hamiltonian now becomes

$$H_0 = -\frac{\hbar^2}{2\mu}\left(\frac{\partial^2}{\partial^2 z_1'^2} + \frac{\partial^2}{\partial^2 z_2'^2}\right) + V(z_1', z_2') , \tag{7}$$

where μ is the same reduced mass as before.

Because the reaction is collinear, the order of the atoms does not change, and the only part of configuration space of interest is the first quadrant in x_1', x_2' space. Not all of the first quadrant is of interest either. Let us define the polar coordinates ρ, α by

$$\rho = (x_2'^2 + x_1'^2)^{\frac{1}{2}} \tag{8a}$$

$$\text{and } \alpha = \tan^{-1}\frac{x_2'}{x_1'} . \tag{8b}$$

The limits of α are at $r_1 = 0$ and $r_2 = 0$. At $r_1 = 0$ we have $\tan\alpha = \frac{m_B}{\mu}$, and at $r_2 = 0$, $\tan\alpha = 0$, so that for H_3, $\alpha_{min} = 0$ and $\alpha_{max} = \pi/3$. Figure 1 shows the Porter and Karplus[6] (PK) H_3 surface in r_1, r_2 coordinates, while Figure 2 shows it in x_1', x_2' coordinates.

In the polar coordinates the Hamiltonian is

$$H_0 = -\frac{\hbar^2}{2\mu}\left(\frac{1}{\rho^2}\frac{\partial^2}{\partial\alpha^2} + \frac{\partial^2}{\partial\rho^2} + \frac{1}{\rho}\frac{\partial}{\partial\rho}\right) + V(\rho,\alpha), \tag{9}$$

and the corresponding Schrödinger equation at energy E is

$$H_0\psi_j(\rho,\alpha) = E\psi_j(\rho,\alpha), \tag{10}$$

where j is an eigenfunction label. If we let

$$\psi_j(\rho,\alpha) = \rho^{-\frac{1}{2}} G_j(\rho,\alpha)$$

the Schrödinger equation becomes

$$-\frac{\hbar^2}{2\mu}\left(\frac{\partial^2 G_j(\rho,\alpha)}{\partial\rho^2} + \frac{1}{\rho^2}\frac{\partial^2 G_j(\rho,\alpha)}{\partial\alpha^2}\right) + \left[V(\rho,\alpha) - \frac{\hbar^2}{8\mu\rho^2}\right]G_j(\rho,\alpha)$$

$$= EG_j(\rho,\alpha). \tag{11}$$

Now let us define a complete, discreet orthonormal set of basis functions $Y_i(\bar{\rho},\alpha)$, such that

$$-\frac{\hbar^2}{2\mu}\frac{d^2 Y_i(\bar{\rho},\alpha)}{d\alpha^2} + \bar{\rho}^2 V(\bar{\rho},\alpha) Y_i(\bar{\rho},\alpha) = \bar{\rho}^2 E_i^{\bar{\rho}} Y_i(\bar{\rho},\alpha), \tag{12}$$

where $Y_j(\bar{\rho},\alpha)$ is parametrically dependent on $\bar{\rho}$. The boundary conditions are $Y_i(\bar{\rho},0) = Y_i(\rho,\alpha_{max}) = 0$. An example of $V(\bar{\rho},\alpha)$ ($\bar{\rho}$ = 5.0 bohr) for the PK H_3 surface is given in figure 4. A corresponding basis function, $Y_i(\bar{\rho},\alpha)$ (i = 7) is also plotted. It is important to note that even at energies above dissociation the eigenfunctions

and eigenvalues are discreet. In other words, we now have a discreet (albeit infinitely large) representation of the continuum. The Y_i's and E_i's are found numerically by a finite difference method, specifically the Givens-Householder[9] method for real symmetric matrices.

If we expand $\psi(\rho,\alpha)$ in terms of these basis functions, we get

$$\psi_j(\rho,\boldsymbol{\alpha}) = \frac{G_j(\rho,\alpha)}{\rho^{\frac{1}{2}}} = \rho^{-\frac{1}{2}} \sum_{i=1}^{\infty} g_{ij}(\rho,\bar{\rho})\, Y_i(\bar{\rho},\alpha)\,, \tag{13}$$

where the g_{ij}'s must depend parametrically on $\bar{\rho}$, although ψ_j does not. Rigorously, the number of terms is infinite, but in practice only a sufficient number are included to achieve a preset degree of convergence. Substituting (12) and (13) into (11) gives

$$-\frac{\hbar^2}{2\mu} \sum_i \frac{d^2 g_{ij}(\rho,\bar{\rho})}{d\rho^2}\, Y_i(\bar{\rho},\alpha) + \frac{\bar{\rho}^2}{\rho^2} \sum_i g_{ij}(\rho,\bar{\rho}) [E_i^{\bar{\rho}} - V(\bar{\rho},\alpha)]\, Y_i(\bar{\rho},\alpha)$$

$$+ [V(\rho,\alpha) - \frac{\hbar^2}{8\mu\rho^2}] \sum_i g_{ij}(\rho,\bar{\rho})\, Y_i(\boldsymbol{\alpha}) = E \sum_i g_{ij}(\rho,\bar{\rho})\, Y_i(\bar{\rho},\alpha). \tag{14}$$

If we left-multiply this equation by $Y_i(\bar{\rho},\alpha)$ and integrate over α, we get the Schrödinger equation in the single variable ρ,

$$-\frac{\hbar^2}{2\mu} g''_{ij}(\rho,\bar{\rho}) + (\frac{\bar{\rho}^2}{\rho^2} E_i^{\bar{\rho}} - \frac{\hbar^2}{8\mu\rho^2} - E)\, g_{ij}(\rho,\bar{\rho})$$

$$+ \sum_{i'} [V_{ii'}(\rho,\bar{\rho}) - \frac{\bar{\rho}^2}{\rho^2} V_{ii'}(\bar{\rho})]\, g_{i'j}(\rho,\bar{\rho}) = 0\,, \tag{15}$$

where

$$V_{ii'}(\rho,\bar{\rho}) = \int_0^{\alpha_{max}} Y_i(\bar{\rho},\alpha)\, V(\rho)\, Y_{i'}(\bar{\rho},\alpha)\, d\alpha .$$

In matrix notation this is written

$$\underset{\approx}{g}'' = \underset{\approx\approx}{U}\underset{\approx}{g} \tag{16}$$

where

$$\underset{\approx}{U} = b\underset{\approx}{V}(\rho,\bar{\rho}) - \frac{b\bar{\rho}^2}{\rho^2}\underset{\approx}{V}(\rho,\bar{\rho}) + \frac{b\bar{\rho}^2}{\rho^2}\underset{\approx}{E} - \left(\frac{1}{4\rho^2} + bE\right)\underset{\approx}{1} \tag{17}$$

and $b = \dfrac{2\mu}{\hbar^2}$.

3. Method of Solution

An efficient method to solve coupled equations of the form of (16) has been developed by Gordon.[4] Given g and g′ at $\rho = \rho_\ell$, the method will find g and g′ at $\rho = \rho_r$. The accuracy is determined by the nature of the potential between ρ_ℓ and ρ_r and the step size $\rho_r - \rho_\ell$. Reducing the step size will improve the accuracy. Briefly, the method approximates $\underset{\approx}{U}(\rho)$ by an analytical reference potential

$$\left[\underset{\approx}{U}_0(\rho)\right]_{ii'} = \left[U_{ii'}(\rho_c) + (\rho - \rho_c)\left.\frac{dU_{ii'}}{d\rho}\right|_{\rho=\rho_c}\right]\delta_{ii'} \tag{18}$$

where ρ_c is the midpoint of ρ_ℓ and ρ_r. The solutions to

$$\underset{\approx}{g}''(\rho) = \underset{\approx}{U}_0(\rho)\,\underset{\approx}{g}(\rho) \tag{19}$$

are Airy functions. Other approximations to the potential could be used; a quadratic approximation has parabolic cylinder functions for solutions; a constant has trigonometric solutions. The linear approximation was chosen as a compromise between efficiency and accuracy. The exact solutions to (16) can now be written as

$$\underset{\approx}{g} = \underset{\approx}{A}\underset{\approx}{a} + \underset{\approx}{B}\underset{\approx}{b} \tag{20a}$$

and

$$\underset{\approx}{g}' = \underset{\approx}{A}'\underset{\approx}{a} + \underset{\approx}{B}'\underset{\approx}{b} \tag{20b}$$

where A and B are the Airy functions solutions of (19) and a and b are slowly varying functions of ρ. Because they are slowly varying, $\underset{\approx}{a}$ and $\underset{\approx}{b}$ are accurately found by the first order expansions

$$\underset{\approx}{a}(\rho_r) = \underset{\approx}{a}(\rho_\ell) + (\rho_r - \rho_\ell)\langle d\underset{\approx}{a}/d\rho\rangle \tag{21a}$$

and

$$\underset{\approx}{b}(\rho_r) = \underset{\approx}{b}(\rho_\ell) + (\rho_r - \rho_\ell)\langle d\underset{\approx}{b}/d\rho\rangle \tag{21b}$$

At very small ρ, $\psi = 0$, which implies that $\underset{\approx}{g} = 0$. We may take $\underset{\approx}{g}' = 1$ at this ρ. Using these initial conditions we then propagate the solution towards larger ρ. When $|\rho - \bar{\rho}|$ is small fewer states are required to describe ψ_j than when the difference is large. In order to keep the number of basis functions to a minimum the basis set is changed periodically as ψ_j is propagated radially. This involves a transformation of the matrix function g and its derivative g'. Suppose we wish to change basis sets at a point ρ. Because ψ_j and its derivative

$\frac{\partial \psi_j}{\partial \rho}$ are both continuous,

$$\sum_{i=1}^{\infty} g_{ij}^{old}(\rho,\bar{\rho})\, Y_i^{old}(\bar{\rho}_{old},\alpha) = \sum_{i=1}^{\infty} g_{ij}^{new}(\rho,\bar{\rho})\, Y_i^{new}(\bar{\rho}_{new},\alpha)$$

and

$$\sum_{i=1}^{\infty} g'^{old}_{ij}(\rho,\bar{\rho})\, Y_i^{old}(\bar{\rho}_{old},\alpha) = \sum_{i=1}^{\infty} g'^{new}_{ij}(\rho,\bar{\rho})\, Y_i^{new}(\bar{\rho}_{new},\alpha).$$

If we left-multiply both sides of each equation by $Y_k^{new}(\bar{\rho}_{new},\alpha)$, integrate over α and recall that the Y_i's are orthonormal, we get

$$\sum_{i=1}^{\infty} g_{ij}^{old}(\rho,\bar{\rho})\, O_{ki}(\bar{\rho}_{new},\bar{\rho}_{old}) = \sum_{i=1}^{\infty} g_{ij}^{new}(\rho,\bar{\rho})\, \delta_{ki}$$

and

$$\sum_{i=1}^{\infty} g'^{old}_{ij}(\rho,\bar{\rho})\, O_{ki}(\bar{\rho}_{new},\bar{\rho}_{old}) = \sum_{i=1}^{\infty} g'^{new}_{ij}(\rho,\bar{\rho})\, \delta_{ki}$$

where

$$O_{ki} = \int Y_k^{new}(\bar{\rho}_{new},\alpha)\, Y_i^{old}(\bar{\rho}_{old},\alpha)\, d\alpha \ .$$

In matrix notation

$$\underset{\approx}{O}\, \underset{\approx}{g}^{old}(\rho,\bar{\rho}) = \underset{\approx}{g}^{new}(\rho,\bar{\rho})$$

$$\underset{\approx}{O}\, \underset{\approx}{g}'^{old}(\rho,\bar{\rho}) = \underset{\approx}{g}'^{new}(\rho,\bar{\rho}) \ .$$

To avoid loss of particle flux, $\underset{\approx}{O}$ should be orthogonal, which is

rigorously satisfied if both the $Y(\bar{\rho}_{old}, \alpha)$ and $Y(\bar{\rho}_{new}, \alpha)$ form complete sets, but is approximately satisfied otherwise. The smaller $\bar{\rho}_{new} - \bar{\rho}_{old}$, the closer $\underset{\approx}{O}$ will be to satisfying this orthogonality condition.

If we examine ψ_j at large ρ, we may expect that is can be written as a sum of three distinct types of functions,

$$\psi_j(\rho,\alpha) \underset{\rho\to\infty}{\approx} \sum_{i=1}^{\infty} g_{ij}\, Y_i(\bar{\rho},\alpha)$$

$$= \sum_{i=1}^{N} g_{ij}^{I}(\rho,\bar{\rho})\, Y_i^{I}(\bar{\rho},\alpha) + \sum_{i=1}^{M} g_{ij}^{II}(\rho,\bar{\rho})\, Y_i^{II}(\bar{\rho},\alpha) + \sum_{i=1}^{\infty} g_{ij}^{III}(\rho,\bar{\rho})\, Y_i^{III}(\bar{\rho},\alpha). \tag{22}$$

The first finite sum describes the system in the A + BC arrangement channel, the second describes the AB + C arrangement channel and the infinite sum describes the dissociated states. A discussion of this partitioning of the wavefunction is in Appendix A.

When the arrangement channels become decoupled (i.e., the elements in the potential matrix coupling different channels become sufficiently small), we switch from the polar coordinates (ρ,α) to the rectangular coordinates (x_1', x_2') and (z_1', z_2') for A + BC and AB + C, respectively. For the dissociative channels we remain in polar coordinates. We perform the change of coordinates because the potential in the bound arrangement channels remains relatively constant, allowing the propagator to take large steps, and reducing, thereby, the computing time. To do this, we must project the wavefunction and its derivative onto a new basis set of the coordinate x_2' (z_2'). Because the wavefunction

and its derivative must be continuous, we have

$$\sum_i h^I_{ij}(x_1', \bar{x}_1')\, \phi^I_i(\bar{x}_1', x_2') = \sum_i g^I_{ij}(\rho, \bar{\rho})\, Y^I_i(\bar{\rho}, \alpha) \tag{23}$$

where h^I_{ij} is a solution of

$$-\frac{\hbar^2}{2\mu} h^{I\prime\prime}_{ij}(x_1', \bar{x}_1') + (E_i^{\bar{x}_1'} - E) h^I_{ij}(x_1', \bar{x}_1') + \sum_{i'} [V_{ii'}(x_1', \bar{x}_1') - V_{ii}(\bar{x}_1')] h^I_{i'j}(x_1', \bar{x}_1') = 0 \tag{24a}$$

and is to be propagated in the coordinate x_1'. ϕ^I_i is a basis function which is a solution of

$$-\frac{\hbar^2}{2\mu} \frac{d^2}{dx_2'^2} \phi^I_i(\bar{x}_1', x_2') + V(\bar{x}_1', x_2')\, \phi^I_i(\bar{x}_1', x_2') = E_i^{\bar{x}_1'} \phi^I_i(\bar{x}_1', x_2'). \tag{24b}$$

Solving for h^I_{ij} we get

$$h^I_{\ell j}(x_1') = \int \sum_m g^I_{mj}(\rho, \bar{\rho})\, Y^I_m(\rho, \alpha)\, \phi^I_\ell(x_2')\, dx_2' \tag{25}$$

where ρ, α are related to x_2' by equations 8a and 8b. Similarly the derivative of the wavefunction must be continuous,

$$\sum_\ell h^{I'}_{\ell j}(x_1')\, \phi^I_\ell(x_2') = \frac{\partial}{\partial x_1'} \sum_\ell g^I_{\ell j}(\rho, \bar{\rho})\, Y^I_\ell(\bar{\rho}, \alpha) \quad .$$

Solving for $h^{I''}_{\ell j}$ gives

$$h^{I'}_{\ell j}(x_1') = \int [\sum_i g^{I'}_{ij}(\rho, \bar{\rho}) \frac{\partial \rho}{\partial x_1'} Y^I_i(\bar{\rho}, \alpha) + g^I_{ij}(\rho, \bar{\rho})\, Y^{I'}_i(\alpha) \frac{\partial \alpha}{\partial x_1'}]\, \phi^I_\ell(x_2')\, dx_2' \tag{26}$$

Similar equations hold for arrangement channel AB + C.

4. Cross Sections

For large ρ, equation (15) takes on the form of a Ricatti-Bessel[5] equation. The jth solution ψ_j is

$$\sum_{n=1}^{N} S^{I}_{nj} \left(\frac{k^{I}_{j}}{k^{I}_{n}}\right)^{\frac{1}{2}} e^{ik^{I}_{n}x'_1} \phi^{I}_{n}(x'_2) + \sum_{n=1}^{M} S^{II}_{nj} \left(\frac{k^{I}_{j}}{k^{II}_{n}}\right)^{\frac{1}{2}} e^{ik^{II}_{n}z'_1} \phi^{II}_{n}(z'_2)$$

$$+ \rho^{-\frac{1}{2}} e^{ik^{III}\rho} \sum_{n=1}^{\infty} S^{III}_{nj} \left(\frac{k_j}{k^{III}}\right)^{\frac{1}{2}} \phi^{III}_{n}(\alpha) + e^{ik^{I}_{j}x'_1} \phi^{I}_{j}(x'_2) \qquad (27)$$

where

$$k^{I}_{n} = \left[\frac{2\mu}{\hbar^2}(E - E^{I}_{n})\right]^{\frac{1}{2}},$$

$$k^{II}_{n} = \left[\frac{2\mu}{\hbar^2}(E - E^{II}_{n})\right]^{\frac{1}{2}},$$

$$k^{III} = \left(\frac{2\mu}{\hbar^2} E\right)^{\frac{1}{2}}$$

and ϕ^{I}_{n}, ϕ^{II}_{n}, ϕ^{III}_{n} are the basis functions for A + BC, AB + C and A + B + C, respectively. ψ_j represents the final scattered system which began in state j of molecule BC and scattered to all other states. The S_{nj}'s are the scattering matrix (S-matrix) elements, and they are calculated in the usual way (see Appendix B).

It is important to note that we have discretized the continuum; the continuum is represented by an infinite sum. The scattering matrix,

although infinite in size, is not continuous. If we make the approximation that the sum can be truncated, we will be able to calculate cross sections for dissociation.

The cross section for reactive and nonreactive scattering is given by

$$\sigma_{nj} = \frac{J_n(Y_1)}{J_j(Y_1')} ,$$

where J_n (J_j) is the total outgoing (incoming) flux in vibrational state n(j) and in direction Y_1 (Y_1'). In physical coordinates x_1, x_2 the flux is given by

$$\underset{\sim}{j}(x_1, x_2) = x_1 \hbar \, \mathrm{Im}\left[\psi^* \frac{1}{\mu_{A,BC}} \frac{\partial \psi}{\partial x_1}\right] + x_2 \hbar \, \mathrm{Im}\left[\psi^* \frac{1}{\mu_{BC}} \frac{\partial \psi}{\partial x_2}\right] . \tag{28}$$

If

$$J(x_1) \equiv \lim_{x_2 \to \infty} \int \underset{\sim}{j}(x_1, x_2) \cdot x_1 \, dx_2$$

then

$$J(x_1) = \lim_{x_2 \to \infty} \frac{\hbar}{2\mu i} \int \left[\psi^* \frac{\partial \psi}{\partial x_1'} - \psi \frac{\partial \psi^*}{\partial x_1'}\right] dx_2' \tag{29}$$

$$= \sum_n |S_{nj}|^2 \cdot \frac{k_j^I \hbar}{\mu} . \tag{30}$$

Therefore, the outgoing flux in state n is given by

$$J_n(x_1) = |S_{nj}|^2 \frac{k_j^I \hbar}{\mu} \tag{31}$$

Since J_j (incoming) $= \frac{\hbar k_j^I}{\mu}$, the nonreactive j→n cross section from A + BC collisions is given by

$$\sigma_{j\to n} = |S_{nj}^I|^2 . \tag{32}$$

Similarly for reaction to arrangement channel II,

$$\sigma_{j\to n} = |S_{nj}^{II}|^2 . \tag{33}$$

For dissociation from an initially bound state, the cross sections are complicated. First we will show that the distribution of energy among the dissociated atoms A, B and C is a function of α.[2b] Let v_2 be the relative velocity of atom A to the center of mass of BC (x_1, x_2 coordinates). Because

$$\frac{x_1}{x_2} = \frac{v_1}{v_2} \quad \text{as} \quad r \to \infty$$

and

$$\tan\alpha = \left(\frac{\mu_{BC}}{\mu_{A,BC}}\right)^{\frac{1}{2}} \frac{x_2}{x_1} ,$$

we get

$$\tan\alpha = \left(\frac{\mu_{BC}}{\mu_{A,BC}}\right)^{\frac{1}{2}} \frac{v_2}{v_1} \quad (\text{as } r \to \infty),$$

where

$$r = (x_1^2 + x_2^2)^{\frac{1}{2}} .$$

From this it follows that

$$v_C = v_1 \left(\frac{m_A}{M}\right) + v_2 \left(\frac{m_B}{m_B + m_C}\right), \tag{34a}$$

$$v_B = v_1 \left(\frac{m_A}{M}\right) - v_2 \left(\frac{m_C}{m_B + m_C}\right), \tag{34b}$$

and that

$$v_A = -v_1 \frac{m_B + m_C}{M}, \tag{34c}$$

where $M = m_A + m_B + m_C$ and v_A, v_B and v_C are the center of mass velocities of atoms A, B, and C, respectively. Because

$$E_T = \tfrac{1}{2}(m_A v_A^2 + m_B v_B^2 + m_C v_C^2)$$

$$= \tfrac{1}{2}(v_1^2 \mu_{A,BC} + v_2^2 \mu_{BC}),$$

the center of mass kinetic energies of atoms A, B and C are given by

$$\frac{E_A}{E_T} = \frac{m_B + m_C}{M} \cos^2 \alpha, \tag{35a}$$

$$\frac{E_B}{E_T} = \frac{m_B}{m_B + m_C} \left[\left(\frac{m_A}{M}\right)^{\frac{1}{2}} \cos\alpha - \left(\frac{m_C}{m_B}\right)^{\frac{1}{2}} \sin\alpha\right]^2 \tag{35b}$$

and

$$\frac{E_C}{E_T} = \frac{m_C}{m_B + m_C} \left[\left(\frac{m_A}{M}\right)^{\frac{1}{2}} \cos\alpha + \left(\frac{m_B}{m_C}\right)^{\frac{1}{2}} \sin\alpha\right]^{\frac{1}{2}} \tag{35c}$$

respectively. Graphs of these ratios versus α are shown in Figure 5.

As one might expect, E_B/E_T is a symmetric function and

$\frac{E_A}{E_T}(\delta) = \frac{E_C}{E_T}(-\delta)$, where $\delta = \alpha - 30°$. The derivations have assumed that $V(\alpha) = 0$ for all α. This assumption is valid in the limit $\rho = \infty$.

Because energy distribution is a function of α, it is useful to find the probability of going from a bound state j to an angle α at $\rho = \infty$. The radial flux beteen α and $\alpha + d\alpha$ is given by

$$\frac{\hbar}{\mu} \operatorname{Im}\left[\psi^* \frac{\partial \psi}{\partial \rho}\right] \rho d\alpha$$

$$= \frac{\hbar}{\mu} k_j \operatorname{Im}\left[i \sum_n \sum_{n'} \phi_n^{III}(\alpha)\, \phi_{n'}^{III}(\alpha)\, S_{nj}^{III*} S_{n'j}^{III}\right] d\alpha. \tag{36}$$

The cross section is

$$\operatorname{Re}\left[\sum_n \sum_{n'} \phi_n^{III}(\alpha)\, \phi_{n'}^{III}(\alpha)\, S_{nj*}^{III} S_{n'j}^{III}\right] d\alpha. \tag{37}$$

For a given total energy E_T, only one of E_A, E_B and E_C is independent. We can, therefore, find the cross section for a particle A having energy between E_A and $E_A - dE_A$. From (35a)

$$E_{A_{max}} = E_T \frac{m_B + m_C}{m_A + m_B + m_C},$$

which implies that

$$E_A/E_{A_{max}} = \cos^2\alpha \qquad \text{or} \qquad \alpha = \cos^{-1}(E_A/E_{A_{max}})^{\frac{1}{2}}.$$

Therefore, the cross section to go from a bound state j to three dissociated atoms with atom A having energy between E_A and $E_A - dE_A$ is

$$\frac{\mathrm{Re}\{\sum_n \sum_{n'} \phi_n^{III}[E_A/E_{A_{max}})^{\frac{1}{2}}]\, \phi_{n'}^{III}[\cos(E_A/E_{A_{max}})^{\frac{1}{2}}] S_{nj}^{III*} S_{n'j}^{III}\}\, dE_A}{2[E_A(E_{A_{max}} - E_A)]^{\frac{1}{2}}}$$

5. Application to the H_3 System

In principle, this method of calculating cross sections is applicable to any collinear atom-diatom system, if the potential surface is known. In choosing a suitable system, we examine several factors. First, the system should be simple. A difficult system, one with a large exothermicity or a deep diatomic potential, might require an excessive number of basis functions for convergence, making it difficult to assess the limitations of the method. Second, for testing this new method, a system for which previous exact results are available should be chosen. Agreement between the results of different methods is a necessary condition for their validity. Third, although it is not essential, it might be useful to use a realistic potential surface. The results might have some physical meaning, particularly if the "true" reaction is dominated by collinear collisions. Finally, it would be very helpful if there are inherent symmetries in the reaction, since such symmetries help us to locate errors and to reduce the computing time. The H_3 surface fits all of the above criteria. In addition, the small masses involved will make the quantum effects more marked.

Although more accurate surfaces are available,[7] we have chosen the Porter Karplus one because this surface is reasonable accurate, is easy to calculate and has been used by previous investigators. The potential does show an anomaly at very small internuclear distances which is, however, easily resolved.*

Before examining the results, it should be noted that in the collinear world, cross sections are dimensionless and equal to probabilities. We will let R denote a reactive transition and N denote a non-reactive transition. For any numerical calculation there are a number of adjustable parameters. Among these are the number of basis functions, the number of points used in calculating the basis functions, and the beginning and end points of the integration. All of the results presented here are converged with respect to these parameters. For example, adding more basis functions does not change the results. (All of the results presented here were calculated using between ten and fourteen basis functions per arrangement channel.) Another criterion of reliability is found in the unitarity condition, $S^{\dagger}S = 1$. We required that the sum of the squares of the absolute values of any column or row of the S matrix be within 1% of unity.

---

*For $\rho < 3.0$ bohr and $\alpha < 3^{\circ}$ (Delves' coordinates) a deep (~ 25 eV) well appears. In fact the potential should be strongly repulsive, and it just set to +30 eV.

First we will compare the values obtained for P_{00}^{R} with those of other workers. In Figure 6, P_{00}^{R} is plotted as a function of energy. The x's are cross sections calculated by Schatz and Kuppermann, the circles are from this work. For low energies ($<.65$ eV) the agreement is excellent. Between the first and second resonances there is some discrepancy. To resolve this, the work by Schatz and Kuppermann was repeated using a finer grid, to calculate the basis functions, and more basis functions (12 instead of 10). The results were invariant with respect to the parameter changes. It was felt that the major difference between the method of reference (1d) and the present work was that Schatz and Kuppermann assumed the dissociative region to be infinitely high while we considered it to have finite value. To examine this difference we allowed Schatz's method to include more of the dissociative region. Again the results were invariant. At present we are unable to resolve or understand this difference in cross sections. For energies above the second resonance, the agreement between the two methods is fair. Overall, one can see that the shapes of the two curves are very similar.

There is some interest in cross sections at very low translational energies. Figure 7 gives a semilog plot of P_{00}^{R} for the results of reference (1d) and the present work. It can be seen that the agreement between them is very good. Using these results we have calculated rate constants for the reactive $0 \rightarrow 0$ transition. The rate constants are given by the formula

$$K_{ij}(T) = (2\mu\pi kT)^{-\frac{1}{2}} \int_{0}^{\infty} P_{ij}^{R}(E_i)\, e^{-E_i/kT}\, dE_i$$

where

$\mu = \mu_{A,BC}$.

k is Boltzmann's constant.

T is the temperature in degrees Kelvin.

E_i is the translational energy of the system with BC in vibrational state v = i.

$P_{ij}^{R}(E_i)$ is the reactive probability from state i to state j.

The range of E_i used in calculating the integral was 0.003 eV to 1.0 eV. Using energies outside of this range did not change the rate constants. They are presented in Table I for a range of temperatures. In Figures 8-13 we present all of the transitions within the range of energies considered (0-1.5 eV translational energy). In the transitions P_{00}^{R}, P_{00}^{V}, P_{01}^{R}, P_{01}^{V}, P_{11}^{R} and P_{11}^{V} we note the strong resonances which occur at the opening of excited vibrational states of H_2.

From the above comparisons, we conclude that this method of calculating collinear transition probabilities is satisfactory and promises to be useful for dissociative collisions. With the general validity of this method established, we will be able to ascertain the importance of closed dissociative eigenfunctions for bound to bound transition probabilities. In addition, we can consider collinear systems which have only a few (3 or 4) bound states, and quickly calculate dissociative cross sections.

APPENDIX A

In this appendix we will discuss the validity of equation (22), i.e.,

$$\psi_j(\rho,\alpha) = \sum_{i=1}^{\infty} g_{ij}\, Y_i(\rho,\alpha)$$

$$= \sum_{i=1}^{M} g^{I}_{ij}(\rho)\, Y^{I}_{i}(\bar{\rho},\alpha) + \sum_{i=1}^{N} g^{II}_{ij}(\rho)\, Y^{II}_{i}(\bar{\rho},\alpha) + \sum_{i=1}^{\infty} g^{III}_{ij}(\rho)\, Y^{III}_{i}(\bar{\rho},\alpha) \tag{A-1}$$

The decoupling of the bound states is relatively straightforward. We expect that because of the nature of the double well in $V(\bar{\rho},\alpha)$ (see Fig. 1), there will be zero spatial overlap between different types of eigenfunctions for sufficiently large ρ. For a nonsymmetric well, this is the case. As $\rho \to \infty$, the bound state eigenfunctions become localized in one well or the other (see Fig. 3). For a symmetric potential, there is no localization at finite ρ. The eigenfunctions are either symmetric or antisymmetric (Fig. 4) and at small ρ (shallow wells) the eigenvalues are not degenerate. As $\rho \to \infty$ (deep wells, wide barrier), the eigenvalues become pairwise degenerate. We can then take linear combinations of the basis functions which are localized. Indeed, since

$$H' Y_i = E_i Y_i$$

and $$H' Y_{i+1} = E_i Y_{i+1}$$

where $$H' = -\frac{\hbar^2}{2\mu\rho^2}\frac{d^2}{dx^2} + V(\bar{\rho},\alpha),$$

we can define Y^{I}_{ℓ} and Y^{II}_{ℓ} by

$$Y_{\ell}^{I} = \frac{1}{\sqrt{2}} (Y_i + Y_{i+1}) \tag{A-2}$$

$$Y_{\ell}^{II} = \frac{1}{\sqrt{2}} (Y_i - Y_{i+1}) , \tag{A-3}$$

where $\ell = i + \frac{1}{2}$. Note that Y_{ℓ}^{I} and Y_{ℓ}^{II} are still eignefunctions of H with eigenvalues E_i. They are localized in the region of arrangement channels $A + BC$ and $AB + C$ respectively. In this way symmetric and antisymmetric eigenfunctions are localized (i.e., decoupled) in the different arrangement channels.

To show that dissociative eigenfunctions decouple from bound eigenfunctions, we must use a different approach. We want to show that

$$V_{ii'}(\rho, \bar{\rho}) - \frac{\bar{\rho}^2}{\rho^2} V_{ii'}(\bar{\rho}) \tag{A-4}$$

[see equation (15)] vanishes. We have shown this to be true for bound eigenfunctions. Because there is no spatial overlap, each of the terms vanishes separately. However, dissociative and bound eigenfunctions do overlap spatially. For simplicity we will consider the matrix element formed by the integral of a symmetric bound function, a symmetric dissociative function and the potential. These will be denoted by $Y^{(S)}$, $Y^{(D)}$ and V, respectively. Let us assume that ρ is always within a neighborhood ϵ of $\bar{\rho}$. That is, $\rho = \bar{\rho} + \epsilon$, where $|\epsilon| < \epsilon_{max}$.

If we expand $V_{ii'}(\rho, \bar{\rho})$ in a Taylor's expansion we get (neglecting higher other terms)

$$V_{ii'}(\bar{\rho} + \epsilon, \bar{\rho}) = V_{ii'}(\bar{\rho}) + V'_{ii}(\bar{\rho}) \cdot \epsilon \ . \tag{A-5}$$

Likewise expanding $\frac{\overline{\rho}^2}{\rho^2}$ gives

$$\frac{\overline{\rho}^2}{\rho^2} = \left[1 - \epsilon/\overline{\rho} + \epsilon^2/\overline{\rho}^2 - \ldots\right]^2 = 1 - 2\epsilon/\overline{\rho} \ . \qquad \text{(A-6)}$$

Substituting (A-5) and (A-6) into (A-4) gives

$$V_{ii'}(\overline{\rho}) + V'_{ii'}(\overline{\rho}) \cdot \epsilon - V_{ii'}(\overline{\rho}) + 2\epsilon/\overline{\rho}\, V_{ii'}(\overline{\rho})$$

$$= V_{ii'}(\overline{\rho}) \cdot \epsilon$$

as $\overline{\rho} \to \infty$. Therefore, to show that (A-4) vanishes, we need only show that $V_{ii'}(\overline{\rho})$ becomes constant asymptotically.

Now

$$V_{ii'}(\rho) = \int_0^{\alpha_{max}} Y^{(S)}\, V(\overline{\rho}, \alpha)\, Y^{(D)}\, d\alpha \ .$$

We will simplify the analysis by considering a symmetric well of the form

$V(\overline{\rho}, \alpha) = \infty$ $\qquad \alpha < 0,\ \alpha > \alpha_{max}$

$V(\overline{\rho}, \alpha) = V_0$ $\qquad 0 < \alpha < \alpha',\ \alpha_{max} - \alpha' < \alpha < \alpha_{max}$

and $V_0 < 0$

$V(\overline{\rho}, \alpha) = 0$ $\qquad$ elsewhere.

The integral now becomes

$$\int_0^{\alpha'} Y^{(S)}\, V_0\, Y^{(D)} d\alpha + \int_{\alpha_{max}-\alpha'}^{\alpha_{max}} = 2\, V_0 \int_0^{\alpha'} Y^{(S)}\, Y^{(D)} d\alpha \ ,$$

since V_0 is constant and the integrand is symmetric. As $\bar{\rho}$ becomes very large, the range of the integral becomes smaller and smaller. When α' becomes sufficiently small, $Y^{(D)}$ will have no oscillations within the range of the integral. The function will become a constant within this range. Meanwhile, the function $Y^{(S)}$ must have oscillations of increasingly larger amplitude. This is because $Y^{(S)}$ is normalized to unity. However, as long as we are using a finite number of dissociative functions, they will become constant before the bound functions become delta functions and we can factor out $Y^{(D)}$. The integral now becomes

$$C'' \int_0^{\alpha'} Y^{(S)} \, d\alpha$$

where C'' is a constant. For the potential we have chosen,

$$Y^{(S)} = A \sin \beta \alpha, \qquad 0 < \alpha < \alpha', \text{ where}$$

$$\beta = \left[\frac{2\mu(E - V_0)}{\hbar^2} \right]^{\frac{1}{2}}.$$

Thus we have, as $\bar{\rho} \to \infty$,

$$V_{ii'}(\bar{\rho}) = C' \int_0^{\alpha'} \sin \beta \alpha \, d\alpha$$

$$= C \cos \beta \alpha'.$$

This does not diverge or oscillate wildly as $\alpha' \to 0$. In fact it converges to a constant C, which is what we wanted to show. Because the integral goes to a constant, we know that

$$V_{ii'}(\rho,\bar{\rho}) - \frac{\rho^2}{\rho^2} V_{ii'}(\bar{\rho})$$

vanishes, that the dissociative part of the wavefunction decouples from the bound part of the wavefunction and therefore that equation (22) is justified.

APPENDIX B

Very far from the origin, the general numerical solution will be

$$\psi_j = \sum_{i=1}^{M} g_{ij}^{I}(x_1')\,\phi_i^{II}(x_2') + \sum_{i=1}^{N} g_{ij}^{II}(z_1')\,\phi_i^{II}(z_2') + \rho^{-\frac{1}{2}} \sum_{i=1}^{L} g_{ij}^{III}(\rho)\,\phi_i^{III}(\alpha), \quad \text{(B-1)}$$

where the g's have the form

$$\begin{aligned} \underset{\approx}{g}^{I} &= \underset{\approx}{\sin} k^{I} x_1' \, \underset{\approx}{B}^{I} + \underset{\approx}{\cos} k^{I} x_1' \, \underset{\approx}{A}^{I} \\ \underset{\approx}{g}^{II} &= \underset{\approx}{\sin} k^{II} z_1' \, \underset{\approx}{B}^{II} + \underset{\approx}{\cos} k^{II} z_1' \, \underset{\approx}{A}^{II} \\ \underset{\approx}{g}^{III} &= \underset{\approx}{\sin} k^{III} \rho \, \underset{\approx}{B}^{III} + \underset{\approx}{\cos} k^{III} \rho \, \underset{\approx}{A}^{III}, \end{aligned} \quad \text{(B-2)}$$

and $\underset{\approx}{\sin} k^{I} x_1'$, $\underset{\approx}{\cos} k^{I} x_1'$ etc. are diagonal matrices of the form

$$\begin{pmatrix} \sin k_1^{I} x_1' & & & \\ & \sin k_2^{I} x_1' & & \\ & & \ddots & \\ & & & \sin k_M^{I} x_1' \end{pmatrix} \quad \text{(B-3)}$$

Because there are $K = L + M + N$ solutions, g^{I} is a $M \times K$ matrix, g^{II} is a $N \times K$ matrix and g^{III} is a $L \times K$ matrix. We can define square $K \times K$ matrices as follows

$$\underset{\approx}{\sin} k\rho = \begin{pmatrix} \underset{\approx}{\sin} k^{I} x_1' & 0 & \\ 0 & \underset{\approx}{\sin} k^{II} z_1' & \\ 0 & 0 & \underset{\approx}{\sin} k^{III} \rho \end{pmatrix} \quad \text{(B-4)}$$

$$\underset{\approx}{g} = \begin{pmatrix} \underset{\approx}{g}^{I} \\ \underset{\approx}{g}^{II} \\ \underset{\approx}{g}^{III} \end{pmatrix} \qquad \underset{\approx}{A} = \begin{pmatrix} \underset{\approx}{A}^{I} \\ \underset{\approx}{A}^{II} \\ \underset{\approx}{A}^{III} \end{pmatrix}$$

Analogous matrices exist for $\underset{\approx}{\cos k\rho}$, $\underset{\approx}{g'}$ and $\underset{\approx}{B}$. We can now write

$$\underset{\approx}{g} = \underset{\approx}{\sin k\rho}\,\underset{\approx}{B} + \underset{\approx}{\cos k\rho}\,\underset{\approx}{A} \tag{B-5}$$

and

$$\underset{\approx}{g'} = \underset{\approx}{k}\,\underset{\approx}{\cos k\rho}\,\underset{\approx}{B} - \underset{\approx}{k}\,\underset{\approx}{\sin k\rho}\,\underset{\approx}{A} \tag{B-6}$$

where $\underset{\approx}{k}$ is the diagonal matrix

$$\begin{pmatrix} k_1^{I} & & & & & & & & \\ & k_2^{I} & & & & & & & \\ & & \ddots & & & & & & \\ & & & k_M^{I} & & & & & \\ & & & & k_1^{II} & & & & \\ & & & & & \ddots & & & \\ & & & & & & k_N^{II} & & \\ & & & & & & & k_1^{III} & \\ & & & & & & & & \ddots \\ & & & & & & & & & k_L^{III} \end{pmatrix}$$

Solving for $\underset{\approx}{A}$ and $\underset{\approx}{B}$ gives

$$\underset{\approx}{A} = \underset{\approx}{\cos k\rho}\,\underset{\approx}{g} - \underset{\approx}{k}^{-1}\,\underset{\approx}{\sin k\rho}\,\underset{\approx}{g'} \tag{B-7}$$

$$\underset{\approx}{B} = \underset{\approx}{\sin k\rho}\,\underset{\approx}{g} + \underset{\approx}{k}^{-1}\,\underset{\approx}{\cos k\rho}\,\underset{\approx}{g'} \; . \tag{B-8}$$

But the physical wavefunction has the form

$$\underset{\approx}{g} = \underset{\approx}{k}^{-\frac{1}{2}}\,(\underset{\approx}{\cos k\rho} + \underset{\approx}{\sin k\rho}\,\underset{\approx}{R}) \tag{B-9}$$

If we take linear combinations of (B-5) to fit it to (B-9) we get

$$\underset{\approx}{g} = (\sin k\rho \underset{\approx}{B} + \cos k\rho \underset{\approx}{A}) \underset{\approx}{P}$$

which implies that

$$\underset{\approx}{A}\underset{\approx}{P} = \underset{\approx}{x}^{-\frac{1}{2}}, \quad \underset{\approx}{B}\underset{\approx}{P} = \underset{\approx}{k}^{-\frac{1}{2}}\underset{\approx}{R}$$

and $$\underset{\approx}{R} = \underset{\approx}{k}^{\frac{1}{2}}\underset{\approx}{B}\underset{\approx}{A}^{-1}\underset{\approx}{k}^{-\frac{1}{2}} .$$

The scattering matrix is given by

$$\underset{\approx}{S} = (\underset{\approx}{1} + i\underset{\approx}{R})(\underset{\approx}{1} - i\underset{\approx}{R})^{-1} .$$

TABLE I

RATE CONSTANTS $k_{oo}(T)$ (cm/molecule-sec)

TEMPERATURE, K	REFERENCE (1d)	THIS WORK
100	4.88 (-4)	5.36 (-4)
200	9.42 (-1)	9.86 (-1)
300	3.16 (1)	3.25 (1)
400	2.23 (2)	2.27 (2)
500	7.73 (2)	7.83 (2)
600	1.83 (3)	1.85 (3)
700	3.47 (3)	3.50 (3)
800	5.66 (3)	5.70 (3)
900	8.37 (3)	8.42 (3)
1000	1.15 (4)	1.16 (4)

References

1. Only a few papers are listed (all on the H_3 surface):
   (a) S. Wu and D. Levine, Molecular Physics, 22 (1971) 881.
   (b) B. Johnson, Chem. Phys. Lett., 13 (1972) 172.
   (c) D. Diestler, J. Chem. Phys., 54 (1971) 4547.
   (d) G. Schatz, J. Bowman and A. Kuppermann, unpublished.
   (e) D. Truhlar and A. Kuppermann, J. Chem. Phys., 56 (1972), 2232.
2. (a) L. Delves, Nuclear Physics, 9 (1959) 391.
   (b) L. Delves, Nuclear Physics, 20 (1960) 275.
3. D. Jepsen and J. O. Hirschfelder, Proc. Nat. Acad. Sci., 45 (1959) 249.
4. R. G. Gordon, J. Chem. Phys., 51 (1969) 14.
5. M. Abramowitz and I. Stegun (ed.), Handbook of Mathematical Functions, (Dover) 1970, p. 445.
6. R. N. Porter and M. Karplus, J. Chem. Phys., 40 (1964) 1105.
7. B. Liu, J. Chem. Phys., 58 (1973) 1925.
8. M. Abramowitz and I. Stegun (ed.), Handbook of Mathematical Functions, (Dover) 1970, p. 361.
9. A. Ralston and H. Wilf (ed.), Mathematical Methods for Digital Computers, Vol. 2, (Wiley) 1967, p. 94.

Figure Captions

Figure 1. The lines are equipotentials of the collinear Porter Karplus H_3 surface in (r_1, r_2) coordinates. The origin of measurement is the dissociated configuration. The dashed lines represent values of the potential for energies below the dissociation energy, while the solid lines are for values above dissociation.

Figure 2. The lines are equipotentials of the collinear PK H_3 surface in (x_1', x_2') coordinates. Units and labeling are indentical to Figure 1.

Figure 3. A cut of the collinear PK DH_2 potential $V(\bar{\rho}, \alpha)$ is plotted at $\bar{\rho} = 5.0$ bohr, with an associated eigenfunction $Y_7(\bar{\rho}, \alpha)$. The abscissa is measured in units of $\alpha_{max} = 50.77°$. The solid horizontal line indicates the position of the corresponding energy.

Figure 4. A cut of the collinear PK H_3 potential $V(\bar{\rho}, \alpha)$ is plotted at $\bar{\rho} = 5.0$ bohr, with an associated eigenfunction $Y_7(\bar{\rho}, \alpha)$. The solid horizontal line indicates the position of the corresponding energy.

Figure 5. Plot of the relative kinetic energy among the dissociated atoms A, B and C, as a function of configuration space in the limit $\rho \to \infty$, for the collinear PK H_3 system.

Figure 6. Plot of the $0 \rightarrow 0$ reactive probability (P_{00}^{R}) calculated by two methods. The x's are from reference (1a). The circles are from the present work. The abscissa is translational energy in eV.

Figure 7. Compares the results from reference (1a) and the present work at low energies, on a semilog scale. The abscissa is translational energy in eV.

Figure 8. Plot of P_{00}^{R} from the present work. The units are the same as in Figre 6. The arrows denote the opening of first and second excited vibrational levels in H_2.

Figure 9. Plot of P_{01}^{R} and P_{02}^{R} from the present work. The units are the same as in Figure 6.

Figure 10. Plot of P_{11}^{R}, P_{12}^{R} and P_{22}^{R} from the present work. The units are the same as in Figure 6.

Figure 11. Plot of P_{00}^{V} from the present work. The units are the same as in Figure 6. The arrows denote the opening of the first and second excited vibrational levels in H_2.

Figure 12. Plot of P_{01}^{V} and P_{02}^{V} from the present work. The units are the same as in Figure 6.

Figure 13. Plot of P_{11}^{V}, P_{12}^{V} and P_{22}^{V} from the present work. The units are the same as in Figure 6.

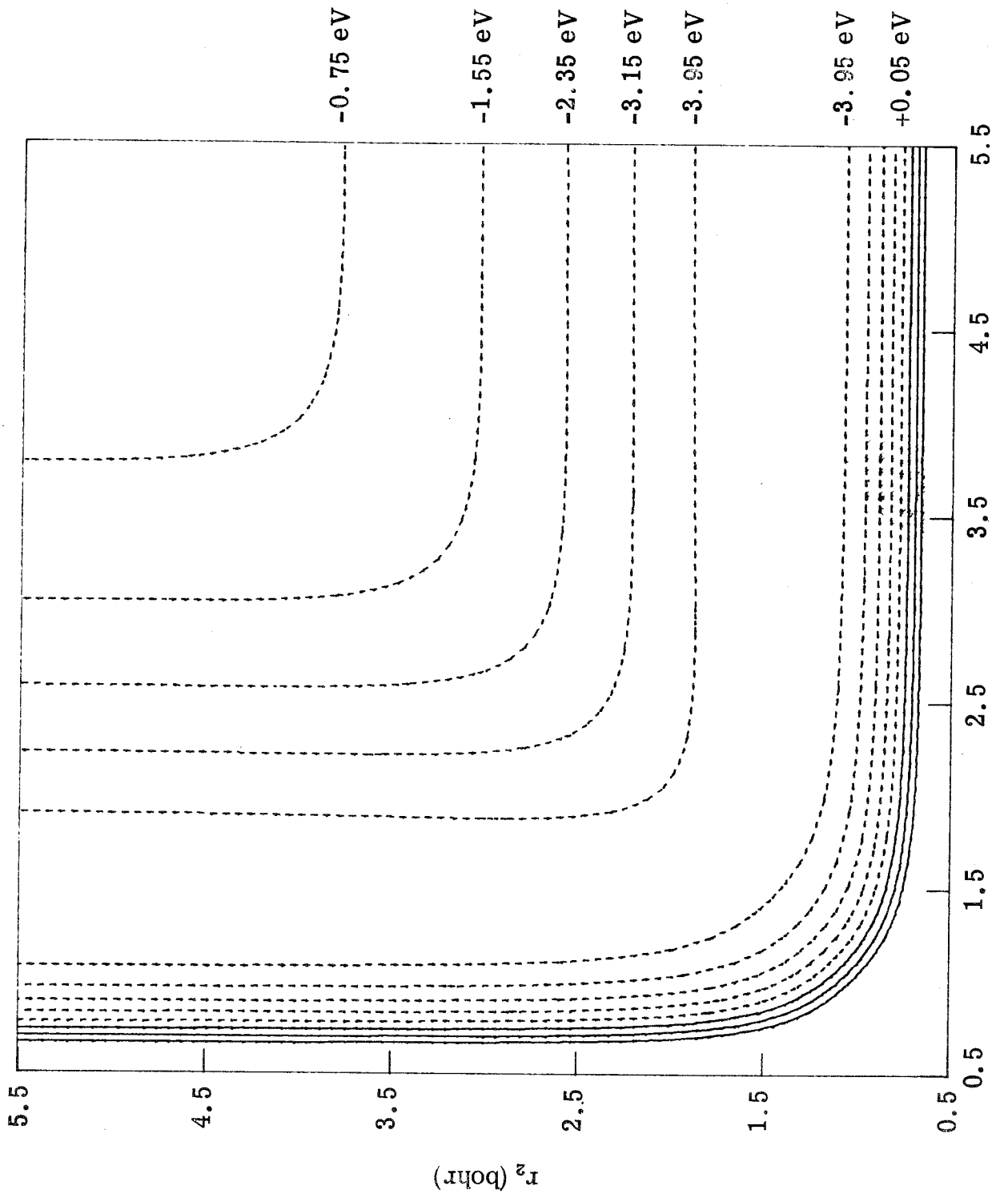
-0.75 eV
-1.55 eV
-2.35 eV
-3.15 eV
-3.95 eV
-3.95 eV
+0.05 eV
5.5
4.5
3.5
2.5
1.5
0.5
r_2 (bohr)
r_1 (bohr)

Figure 1

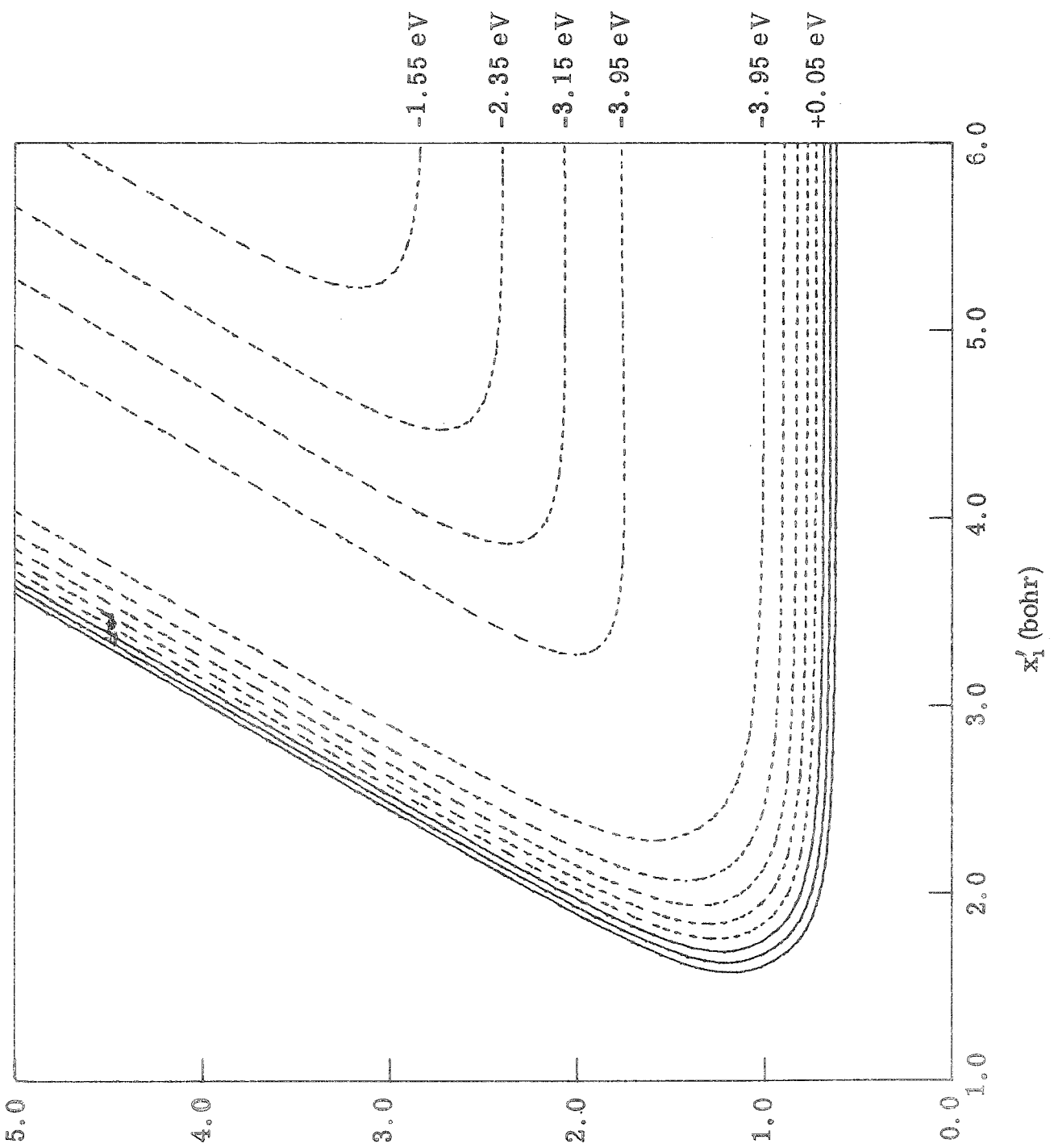
-1.55 eV
-2.35 eV
-3.15 eV
-3.95 eV
-3.95 eV
+0.05 eV
5.0
4.0
3.0
2.0
1.0
0.0
1.0
2.0
3.0
4.0
5.0
6.0
x_2' (bohr)
x_1' (bohr)

Figure 2

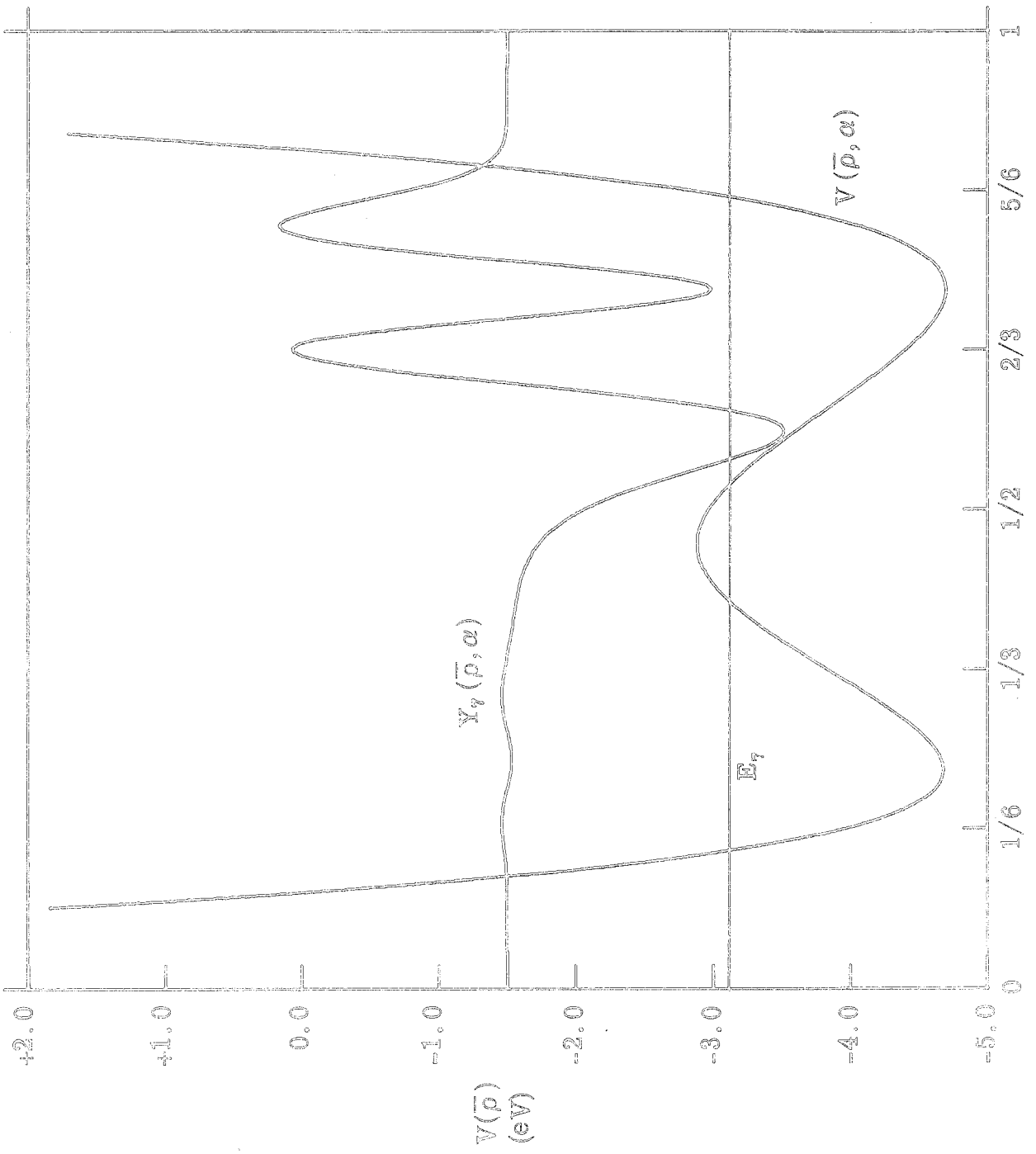

Figure 3

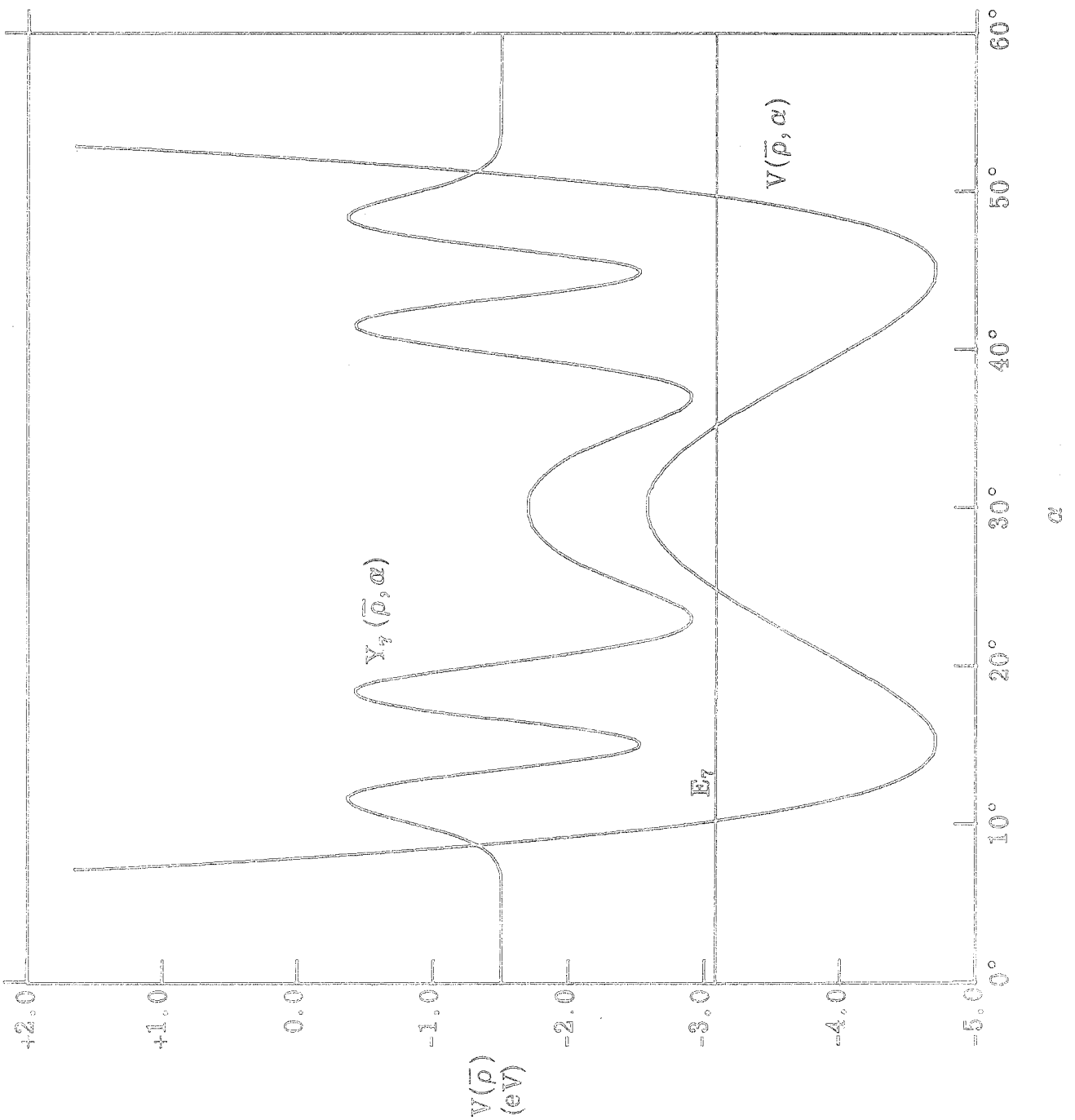
+2.0
+1.0
0.0
-1.0
-2.0
-3.0
-4.0
-5.0
V(ρ) (eV)
10°
20°
30°
40°
50°
60°
α
Ef
$V(\bar{\rho},\alpha)$
$\chi_4(\bar{\rho},\alpha)$

Figure 4

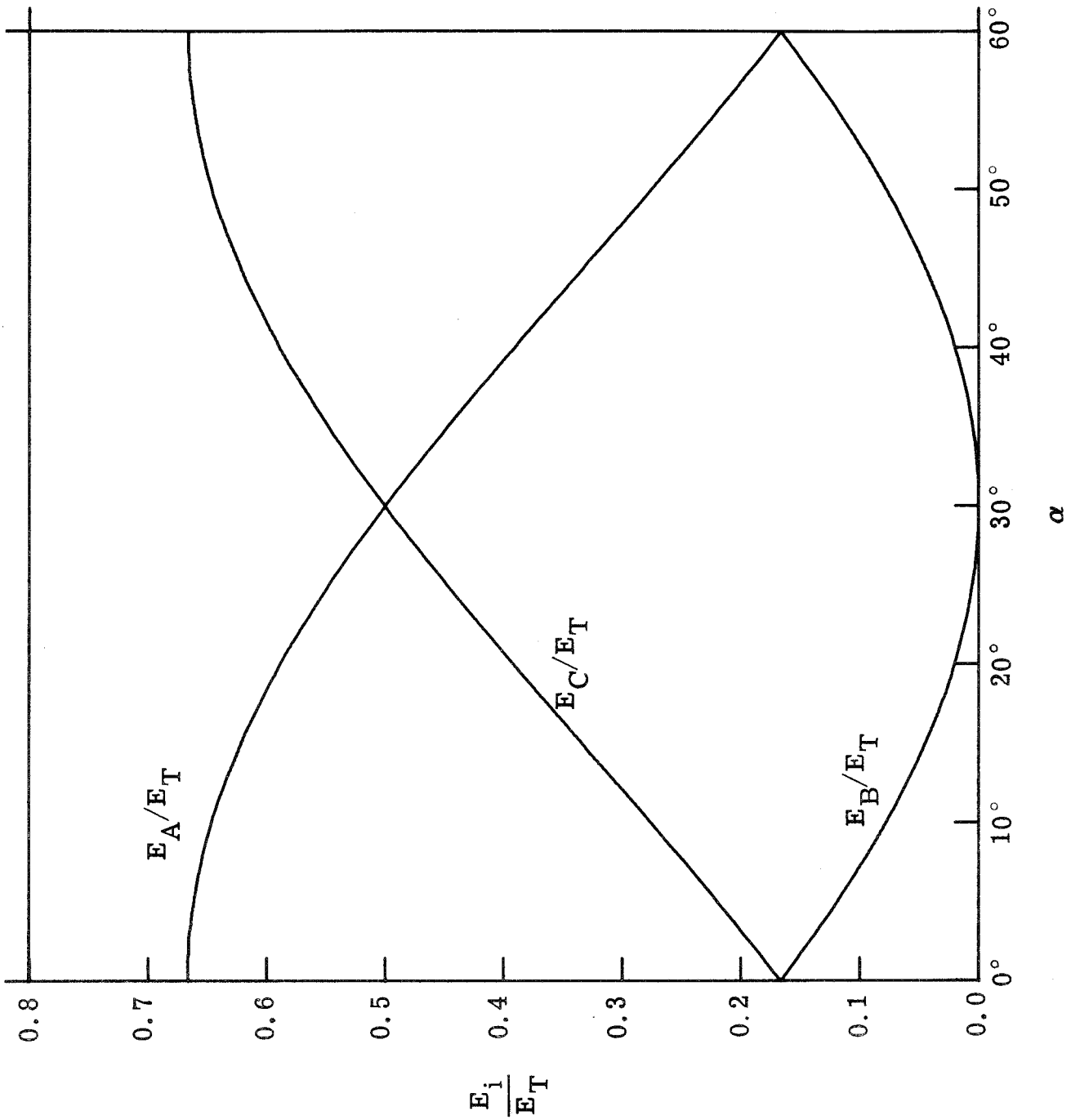
E_A/E_T
E_C/E_T
E_B/E_T
$\frac{E_i}{E_T}$
0.0
0.1
0.2
0.3
0.4
0.5
0.6
0.7
0.8
0°
10°
20°
30°
40°
50°
60°
α

Figure 5

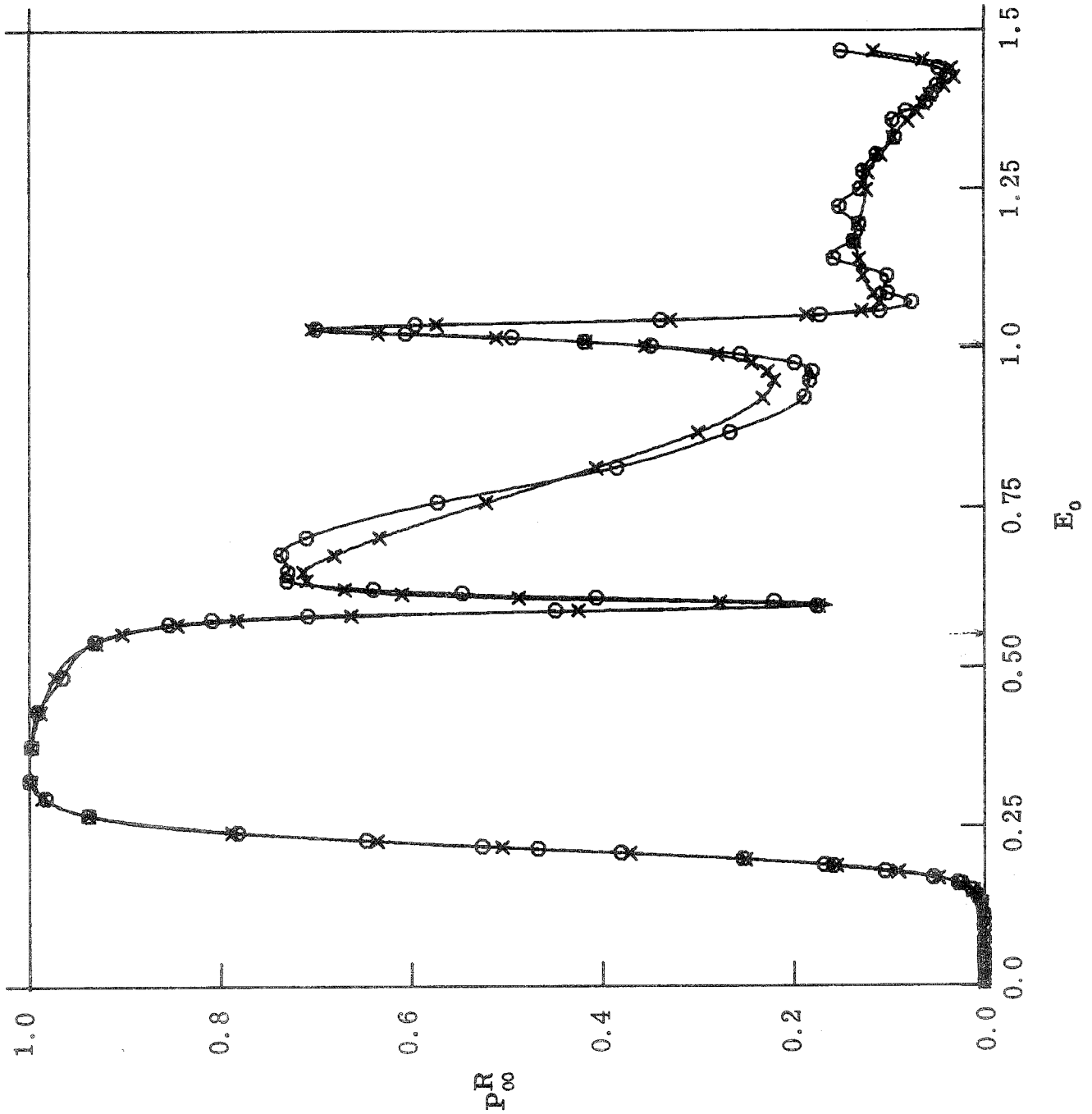

Figure 6

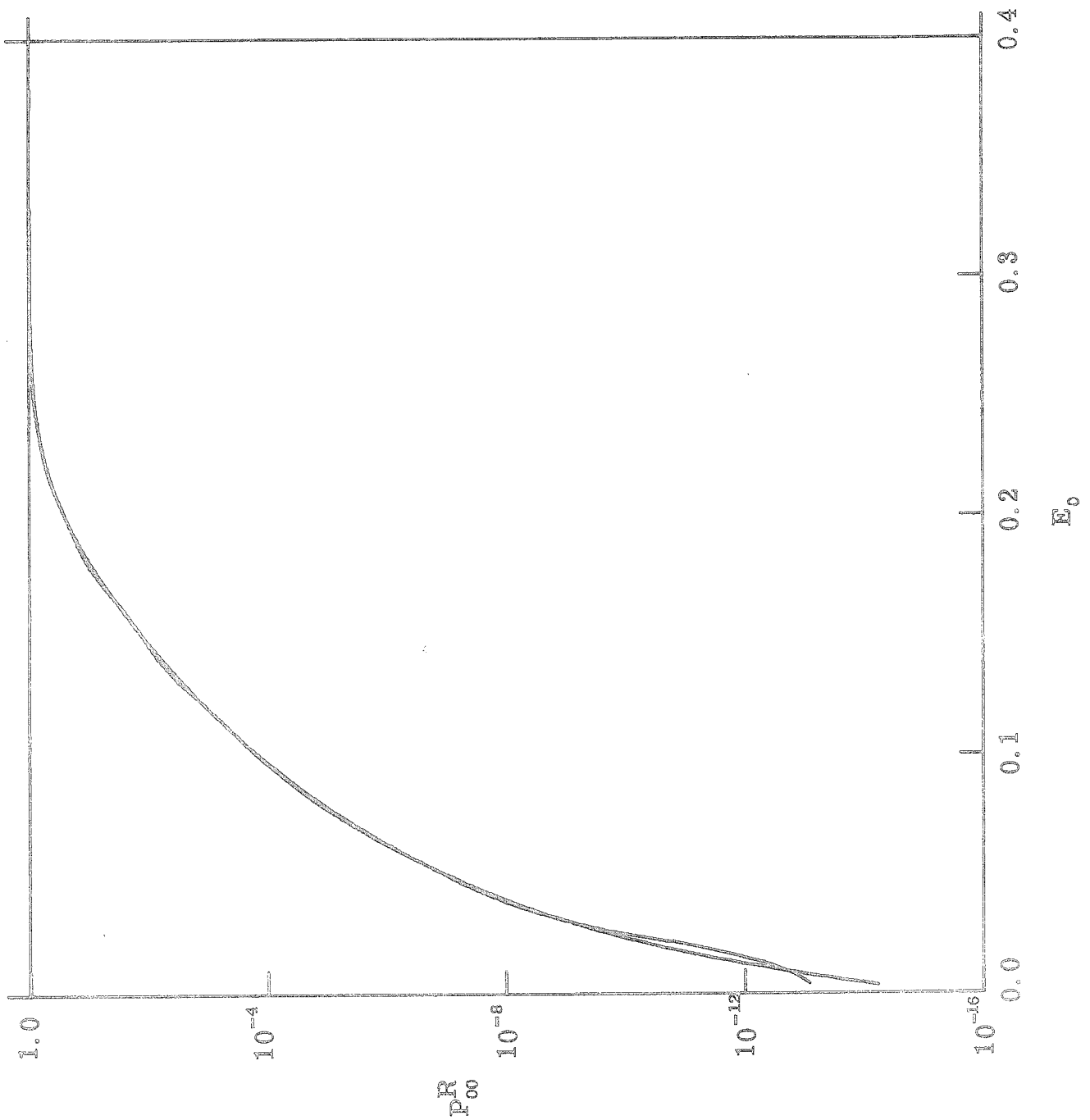

Figure 7

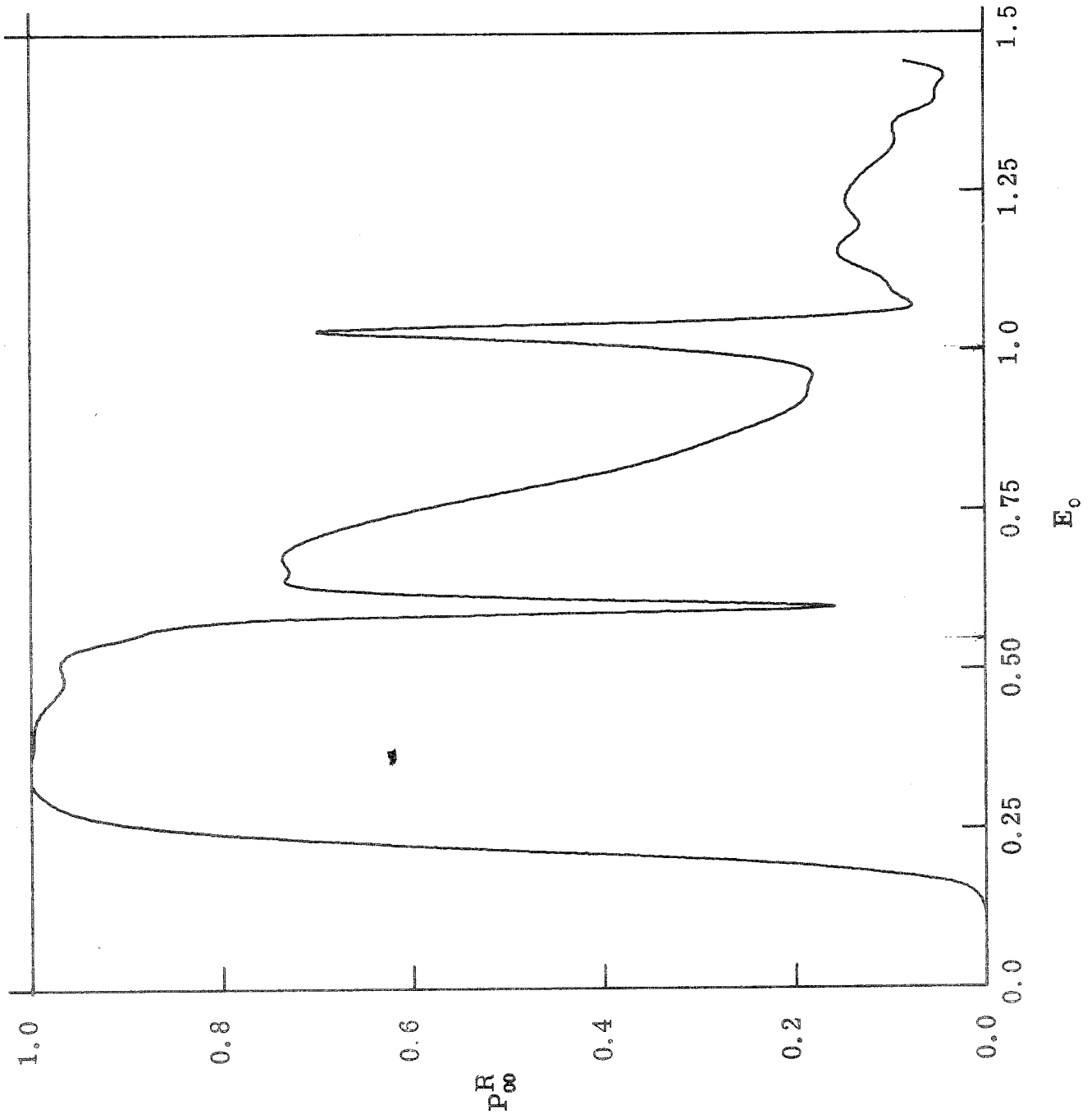

Figure 8

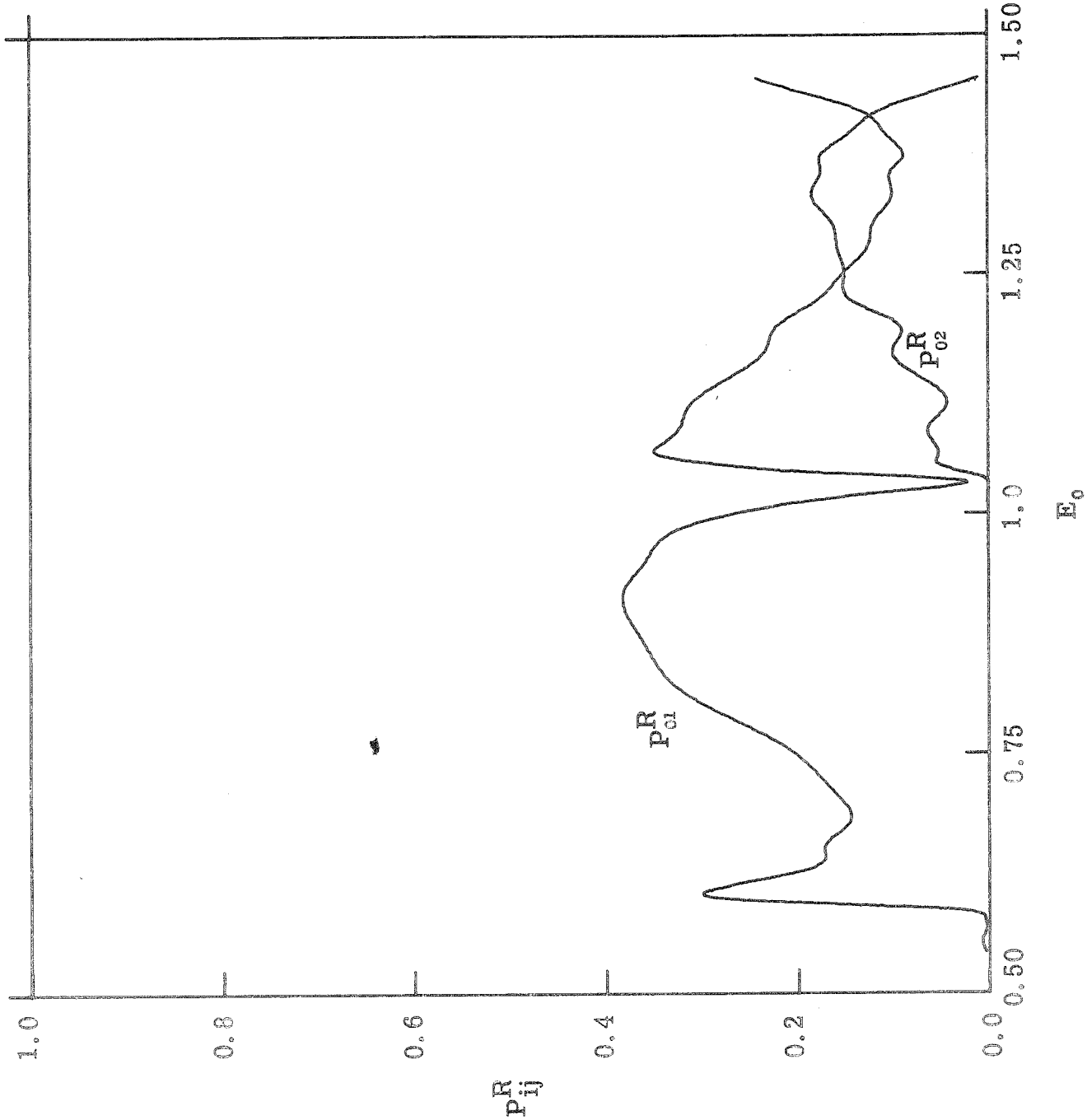

Figure 9

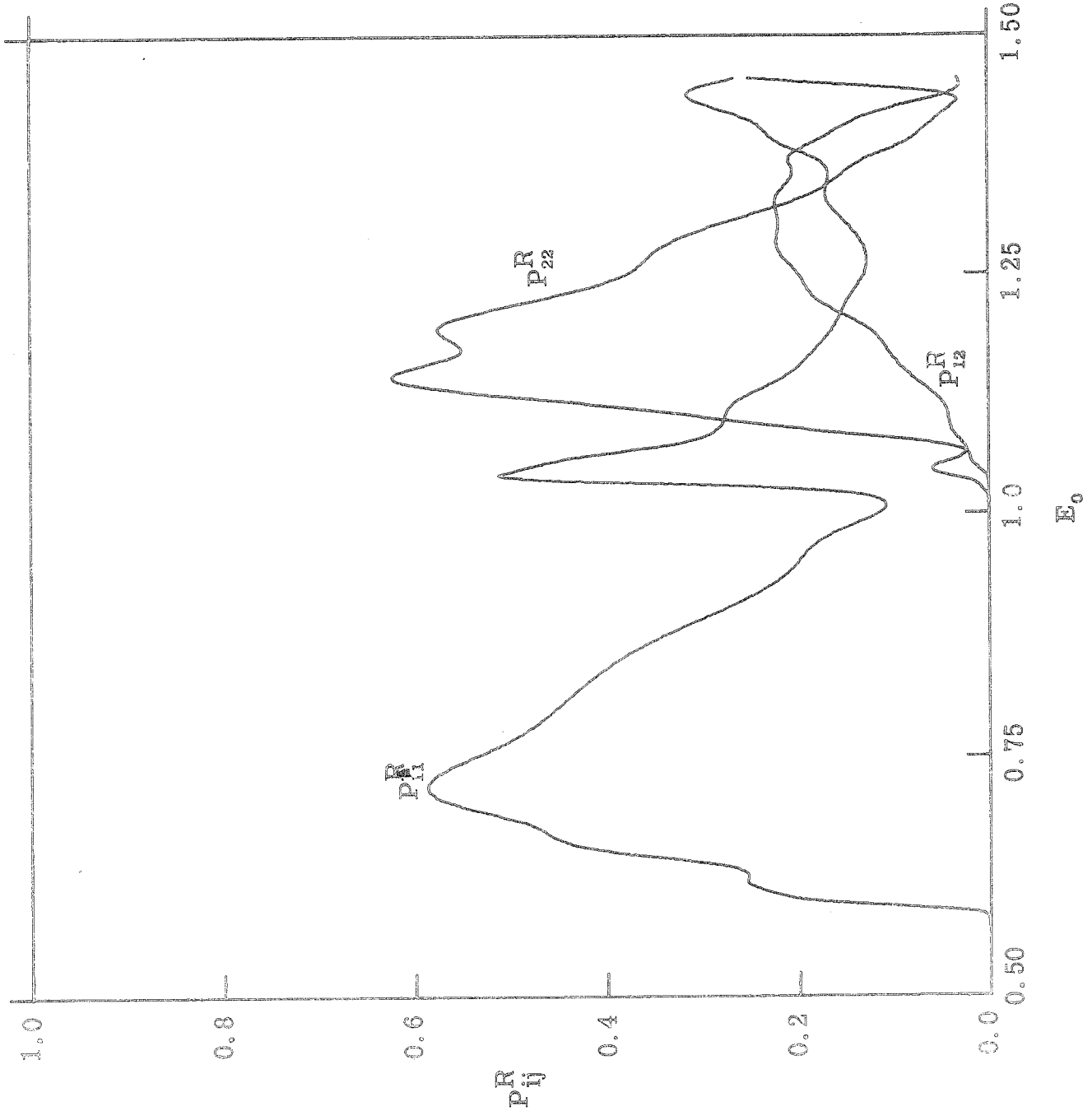

Figure 10

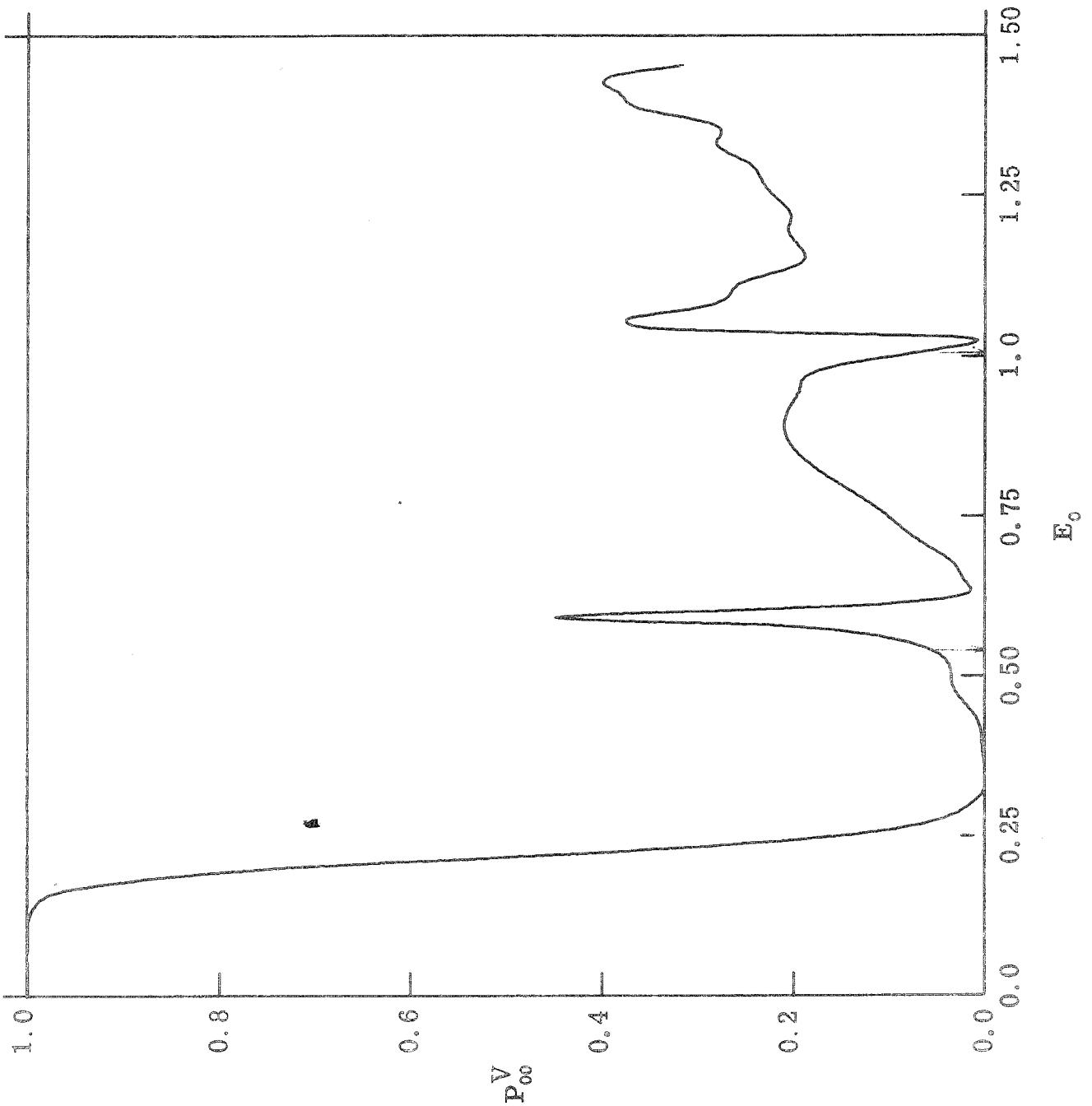

Figure 11

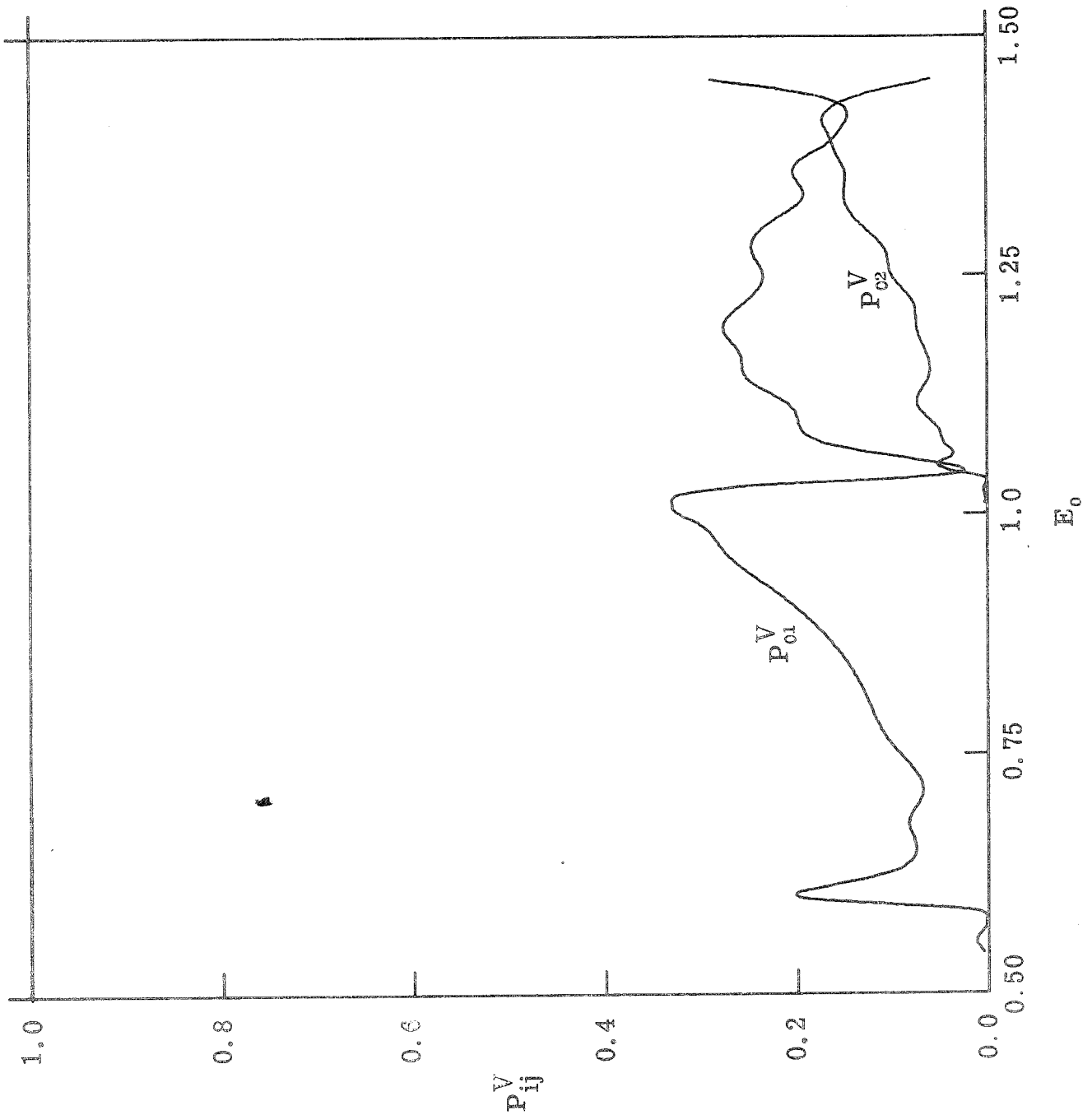

Figure 12

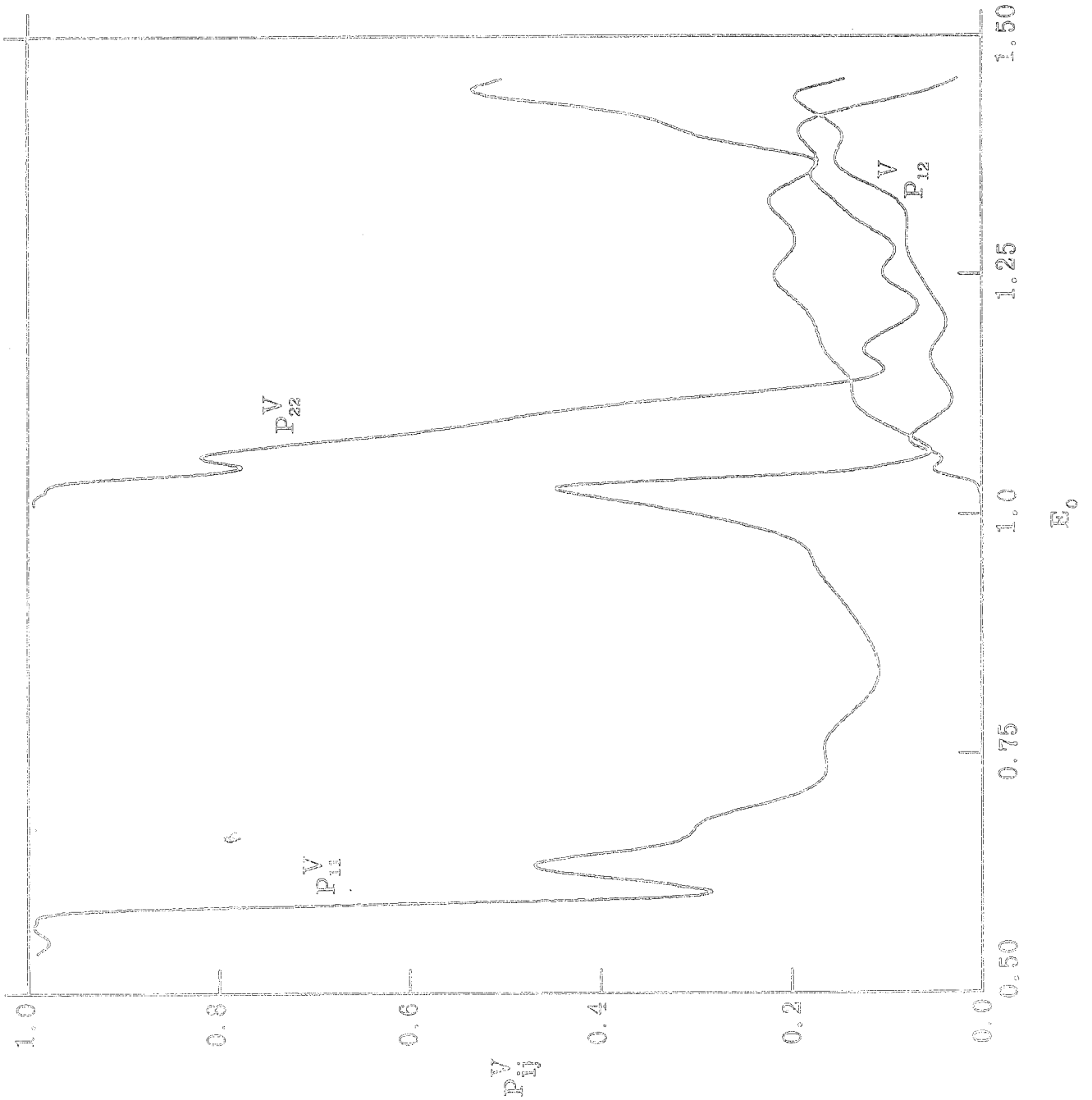
1.50
1.25
1.0
0.75
0.50
0.0
0.2
0.4
0.6
0.8
1.0
P_{12}^{V}
P_{22}^{V}
P_{11}^{V}
P_{12}^{V}
P_{22}^{V}
P_{11}^{V}
ξ_2

Figure 13

PART II

1. Introduction

In a recent paper[1] Clarke and Thiele reported vibrational-vibrational (V-V) and translational-vibrational (T-V) transition probabilities for the collinear collision of two identical harmonic oscillators interacting via an exponentially repulsive potential. After reducing the problem to a pseudo atom-diatom collision (using a method developed by Zelechow[2] et al.), they used the adiabatic approximation of Thiele and Katz[5] and the first order distorted wave T and K matrix methods to calculate transition probabilities. They compared their results to the exact quantum calculations of Riley and Kuppermann[3] and concluded that only two of the "exact" probabilities are correct. We have calculated the exact quantum mechanical transition probabilities using the method of Riley and Kuppermann, but using a larger basis set. We conclude that neither the results of Clarke and Thiele nor the results of Riley and Kuppermann are completely accurate.

2. Equations

We will briefly develop the equations to be solved. A more complete treatment is given by Riley.[4] Consider the collinear collision of two diatomic molecules AB and CD, where B and C are the nearest end atoms. Let z_i and m_i be the laboratory coordinate and mass respectively of particle i. The Hamiltonian for this system is

$$-\frac{\hbar}{2}\sum_i \frac{1}{m_i}\frac{\partial^2}{\partial z_i^2} + V_{CD}(|z_C - z_D|) + V_{AB}(|z_A - z_B|)$$

$$+ V_I(|z_B - z_C|) .$$

We have assumed that the potential consists of three parts. The first two depend on the internuclear distances of molecules AB and CD respectively; the third depends on the nearest end atom separation. If we let

$$x = |z_A - z_B|$$

$$y = |z_C - z_D|$$

$$\mathcal{R} = (m_A z_A + m_B z_B + m_C z_C + m_D z_D)/M ,$$

$$\text{where } M = m_A + m_B + m_C + m_D ,$$

we can factor out the center of mass coordinate $\mathcal{R}$. We now introduce harmonic oscillator potentials. That is,

$$V_{AB} = \tfrac{1}{2}K_{AB}(x - x_{eq})^2$$

$$V_{CD} = \tfrac{1}{2}K_{CD}(y - y_{eq})^2 ,$$

where K_{AB} and K_{CD} are the force constants and x_{eq} and y_{eq} are the equilibrium distances of AB and CD respectively. If we define

$$\bar{y} = \left(\frac{\mu_{CD} \cdot K_{CD}}{\hbar^2}\right)^{\frac{1}{4}} \cdot (y - y_{eq})$$

$$\bar{x} = \left(\frac{\mu_{AB} \cdot K_{AB}}{\hbar^2}\right)^{\frac{1}{4}} \cdot (x - x_{eq})$$

$$\omega_{CD} = (K_{CD}/\mu_{CD})^{\frac{1}{2}}$$

$$\omega_{AB} = (K_{AB}/\mu_{AB})^{\frac{1}{2}}$$

where

$$\mu_{AB} = \frac{m_A \cdot m_B}{m_A + m_B}$$

$$\mu_{CD} = \frac{m_C \cdot m_D}{m_C + m_D}$$

$$\gamma_{AB} = \frac{\mu_{AB}}{m_B}$$

$$\gamma_{CD} = \frac{\mu_{CD}}{m_C}$$

$$\mu = \frac{(m_A + m_B)(m_C + m_D)}{M},$$

the Schrödinger equation becomes

$$\left[-\tfrac{1}{2}\hbar\omega_{CD}\left(-\frac{\partial^2}{\partial\bar{y}^2}+\bar{y}^2\right)-\tfrac{1}{2}\hbar\omega_{AB}\left(-\frac{\partial^2}{\partial\bar{x}^2}+\bar{x}^2\right)\right.$$

$$\left.+\frac{\hbar^2}{2\mu}\frac{\partial^2}{\partial r^2}+V_I(r-\gamma_{AB}\bar{x}+\gamma_{CD}\bar{y})-E\right]\psi(\bar{x},\bar{y},r)=0.$$

The interaction between B and C is chosen as

$$V_I(|z_B-z_C|)=e^{-|z_B-z_C|/L},$$

where L is a characteristic length. We now define

$$\bar{E}=2E/\hbar\omega_{CD} \qquad m=\frac{(m_A+m_B)m_D}{m_C M}$$

$$\bar{\omega}=\omega_{AB}/\omega_{CD} \qquad \alpha=\frac{1}{L}\gamma_{CD}\left(\frac{\hbar^2}{\mu_{CD}K_{CD}}\right)^{\frac{1}{4}}$$

$$\bar{r}=\frac{1}{\gamma_{CD}}\left(\frac{\mu_{CD}K_{CD}}{\hbar^2}\right)^{\frac{1}{4}}r \qquad \beta=\frac{\gamma_{AB}}{\gamma_{CD}}\left(\frac{\mu_{CD}K_{CD}}{\mu_{AB}K_{AB}}\right)^{\frac{1}{4}}.$$

The final form of the Schrödinger equation becomes

$$\left[\left(-\frac{\partial^2}{\partial y^2}+y^2\right)+\omega\left(-\frac{\partial^2}{\partial x^2}+x^2\right)-\frac{1}{m}\frac{\partial^2}{\partial r^2}\right.$$

$$\left.+\exp\{-\alpha(r-y-\beta x)\}-E\right]\psi(x,y,r)=0.$$

Note that the bars on all variables have been dropped for simplicity.

Let

$$H_0(x,y) = -\frac{\partial^2}{\partial y^2} + y^2 + \omega\left(-\frac{\partial^2}{\partial x^2} + x^2\right) .$$

The eigenfunctions of $H_0(x,y)$ are given by

$$H_0(x,y)\,\Phi_{ij}(x,y) = W_{ij}\,\Phi_{ij}(x,y) \qquad i,j = 0,1,2,\ldots ,$$

where

$$\Phi_{ij}(x,y) = \phi_i(y)\,\phi_j(x)$$

and

$$W_{ij} = (2i+1) + \omega(2j+1) .$$

The complete wavefunction is given by

$$\psi^{n'm'}(x,y,r) = \sum_{n=0}^{N-1}\sum_{m=0}^{M-1} f_{nm}^{n'm'}(r)\,\phi_n(y)\,\phi_m(x) ,$$

where n' and m' are the initial quantum numbers and N and M are the number of eigenstates in the expansion for coordinates y and x respectively. This is an exact wavefunction for all energies as $N,M \rightarrow \infty$. However, for numerical calculations, N and M are chosen to be finite, say $N = n$, $M = m$. The transiton probabilities are considered to be converged when $N = n + 1$ and $M = m + 1$ produce no significant change.

3. Parameters

Following Riley and Kuppermann and Clarke and Thiele we have chosen the following values for the parameters ω, β, m, α:

$$\omega = 1$$

$$\beta = 1$$

$$m = .5 \text{ (from } m_A = m_B = m_C = m_D = 1)$$

$$\alpha = 0.2973$$

All other parameters (starting point of integration, etc.) were identical to those of reference (4). $m_A = m_B = m_C = m_D$ means that AB and CD are identical homonuclear diatomics. $\beta = 1$ and $\omega = 1$ imply that the internal potentials are identical.

4. Method

We have used Riley's method and program (DRILL) to calculate transition probabilities at various energies. Briefly, the method is an integration of the Schrödinger equation with reorthogonalization of the radial wavefunction. This reorthogonalization is necessary because some columns of the radial function (which is a matrix) become linearly dependent. If $\underset{\approx}{f}(r)$ is the radial matrix wavefunction, then the function and its derivative after reorthogonalization are given by

$$\underset{\approx}{f}^{new}(r) = \underset{\approx}{f}^{old}(r)\,\underset{\approx}{C}$$

$$\underset{\approx}{f}^{new}(r) = \underset{\approx}{f}^{old}(r)\,\underset{\approx}{C}$$

The obvious choice for $\underset{\approx}{\mathscr{C}}$ is $\underset{\approx}{f}^{-1}(r)$. This procedure is used at regular intervals. In his expansion Riley used M = N = 3 for all energies considered. In order to prove convergence we have used four-, five- and six-state expansions.

5. Results and Discussion

The results for five and six state expansions are presented in Tables I and II for a variety of energies. Included are the results of Riley and Kuppermann (M = N = 3) and Clarke and Thiele. In their paper Clarke and Thiele present a partial decoupling scheme which reduces the problem to a pseudo atom-diatom collision. Although they used approximate methods to calculate transition probabilities, they showed rigorously that

$$\frac{P_{00 \rightarrow 11}}{P_{00 \rightarrow 02}} = 2 ,$$

where $P_{ij \rightarrow k\ell}$ is the probability of going from the ij state to the $k\ell$ state. On the basis of this result they were able to conclude that certain of the transition probabilities calculated by Riley and Kuppermann are incorrect. Table III lists this ratio for various M, N. First note that the results in Tables I and II are nearly identical for N = M = 5 and N = M = 6. The largest discrepancy is 1 part in 2000. In addition Table II shows that the ratio $P_{00 \rightarrow 11}/P_{00 \rightarrow 02}$ has converged to 2 as predicted by Clarke and Thiele. From this we conclude that our results are correct. At the lowest energies (4.1, 4.5) the adiabatic results are

accurate to about 1% or better. At those transitions for which 6.1 is the lowest energy, the agreement is still excellent. For all but the highest energy, the accuracy is better than 10%.

For V-V transition the results of Riley and Kuppermann are in good agreement with ours for the lowest transition (01 → 10). As expected the agreement is somewhat worse for higher transitions except at E = 6.1. For T-V transitions, the agreement is good only for the lowest energies (4.1, 4.5, 5.0, 5.5) of the lowest transition.

Although direct integration of the Schrödinger equation is not an entirely satisfactory method of solving quantum problems, it does provide an opportunity to test approximate methods. In fact we have seen that the adiabatic method of Thiele and Katz gives results in good agreement (error less than 10%) for all but the highest collision energies. In addition, one should note the importance of the theorem of Clarke and Thiele, which predicts the ratio of two of the transition probabilities. This theorem, which we have numerically verified, gives one a measure of the reliability of the calculated results. Without such a test, one might incorrectly conclude that the calculated transition probabilities are accurate.

Table I. Transition probabilities for 1 and 2 quanta V-V energy transfer.

Transition	E	Riley and Kuppermann	Clarke and Thiele†	This Work M = N = 5	This Work M = N = 6
01 → 10	4.1	0.41×10^{-2}	0.41×10^{-2}	0.4100×10^{-2}	
	4.5	0.2109×10^{-1}	0.2094×10^{-1}	0.2109×10^{-1}	0.2109×10^{-1}
	5.0	0.4376×10^{-1}	0.4285×10^{-1}	0.4376×10^{-1}	0.4376×10^{-1}
	5.5	0.6805×10^{-1}	0.6545×10^{-1}	0.6808×10^{-1}	0.6808×10^{-1}
	6.1	0.9894×10^{-1}	0.9319×10^{-1}	0.9924×10^{-1}	0.9924×10^{-1}
	7.0	0.1459	0.1371	0.1483	0.1483
	7.9	0.1875	0.1780	0.1957	0.1957
02 → 11	6.1	0.7821×10^{-2}	0.7843×10^{-2}	0.7850×10^{-2}	0.7850×10^{-2}
	7.0	0.7609×10^{-1}	0.7882×10^{-1}	0.8033×10^{-1}	0.8033×0^{-1}
	7.9	0.1317	0.1480	0.1544	0.1544
02 → 20	6.1	0.1695×10^{-4}	0.1710×10^{-4}	0.1711×10^{-4}	0.1711×10^{-4}
	7.0	0.1571×10^{-2}	0.1707×10^{-2}	0.1780×10^{-2}	0.1780×10^{-2}
	7.9	0.5165×10^{-2}	0.6508×10^{-2}	0.7248×10^{-2}	0.7248×10^{-2}

†These results are calculated using the adiabatic method of Thiele and Katz.

Table II. Transition probabilities for 1 and 2 quanta T-V energy transfer.

Transition	E	Riley and Kuppermann	Clarke and Thiele†	This Work M = N = 5	This Work M = N = 6
00 → 01	4.1	0.169×10^{-5}	0.167×10^{-5}	0.1665×10^{-5}	
	4.5	0.784×10^{-4}	0.802×10^{-4}	0.7883×10^{-4}	0.7884×10^{-4}
	5.0	0.650×10^{-3}	0.672×10^{-3}	0.6503×10^{-3}	0.6503×10^{-3}
	5.5	0.231×10^{-2}	0.244×10^{-2}	0.2325×10^{-2}	0.2325×10^{-2}
	6.1	0.641×10^{-2}	0.701×10^{-2}	0.6568×10^{-2}	0.6568×10^{-2}
	7.0	0.174×10^{-1}	0.207×10^{-1}	0.1879×10^{-1}	0.1879×10^{-1}
	7.9	0.326×10^{-1}	0.439×10^{-1}	0.3854×10^{-1}	0.3854×10^{-1}
01 → 11	6.1	0.195×10^{-5}	0.169×10^{-5}	0.1691×10^{-5}	0.1691×10^{-5}
	7.0	0.826×10^{-3}	0.675×10^{-3}	0.6513×10^{-3}	0.6512×10^{-3}
	7.9	0.653×10^{-2}	0.514×10^{-2}	0.4745×10^{-2}	0.4745×10^{-2}
01 → 02	6.1	0.111×10^{-5}	0.324×10^{-5}	0.3238×10^{-5}	0.3237×10^{-5}
	7.0	0.152×10^{-5}	0.128×10^{-2}	0.1188×10^{-2}	0.1188×10^{-2}
	7.9	0.444×10^{-3}	0.122×10^{-1}	0.8269×10^{-2}	0.8270×10^{-2}

Table II (Cont.)

Transition	E	Riley and Kuppermann	Clarke and Thiele†	This Work M = N = 5	This Work M = N = 6
01 → 20	6.1	0.56×10^{-7}	0.115×10^{-6}	0.1216×10^{-6}	0.1216×10^{-6}
	7.0	0.455×10^{-4}	0.629×10^{-4}	0.1139×10^{-3}	0.1139×10^{-3}
	7.9	0.413×10^{-3}	0.258×10^{-2}	0.1314×10^{-2}	0.1314×10^{-2}
00 → 11	6.1	0.15×10^{-7}	0.998×10^{-8}	0.1128×10^{-7}	0.1128×10^{-7}
	7.0	0.224×10^{-4}	0.989×10^{-5}	0.1262×10^{-4}	0.1262×10^{-4}
	7.9	0.397×10^{-3}	0.120×10^{-3}	0.1945×10^{-3}	0.1944×10^{-3}
00 → 02	6.1	0.35×10^{-8}	0.494×10^{-8}	0.5638×10^{-8}	0.5639×10^{-8}
	7.0	0.189×10^{-5}	0.494×10^{-5}	0.6308×10^{-5}	0.6309×10^{-5}
	7.9	0.181×10^{-4}	0.599×10^{-4}	0.9720×10^{-4}	0.9722×10^{-4}

†These results are calculated using the adiabatic method of Thiele and Katz, except for the 00 → 11 and 00 → 02 transitions. These are "corrected" adiabatic results.

Table III. $\frac{P_{00 \rightarrow 11}}{P_{00 \rightarrow 02}}$

E	Riley and Kuppermann	M = N = 4	M = N = 5	M = N = 6
6.1	4.314	1.998	2.000	2.000
7.0	11.84	2.012	2.001	2.000
7.9	21.96	2.185	2.000	2.000

References

1. J. Clarke and E. Thiele, Chem. Phys., 4, (1974) 447.
2. A. Zelechow, D. Rapp and T. Sharp, J. Chem. Phys., 48 (1968) 286.
3. M. Riley and A. Kuppermann, Chem. Phys. Letters 1, (1968) 537.
4. M. Riley, Ph.D. Thesis, California Institute of Technology (1968).
5. E. Thiele and R. Katz, J. Chem. Phys., 55, (1971) 3195.